Carbones and Carbon Atom as Ligands in Transition Metal Complexes

Lili Zhao[a], Chaoqun Chai[a], Wolfgang Petz*[b], Gernot Frenking*[a,b]

[a]Institute of Advanced Synthesis, School of Chemistry and Molecular Engineering, Jiangsu National Synergetic Innovation Center for Advanced Materials, Nanjing Tech University, Nanjing 211816, China.

[b]Fachbereich Chemie, Philipps-Universität Marburg, Hans-Meerwein-Strasse 4, D-35043 Marburg, Germany.

Email: petz@staff.uni-marburg.de; frenking@chemie.uni-marburg.de

Abstract: This review summarizes experimental and theoretical studies of transition metal complexes with two types of novel metal-carbon bonds. One type features complexes with carbones CL_2 as ligands, where the carbon(0) atom has two electron lone pairs which engage in double (σ and π) donation to the metal atom $[M]\leftleftharpoons CL_2$. The second part of this review reports complexes which have a neutral carbon atom C as ligand. Carbido complexes with naked carbon atoms may be considered as endpoint of the series $[M]\text{-}CR_3 \rightarrow [M]\text{-}CR_2 \rightarrow [M]\text{-}CR \rightarrow [M]\text{-}C$.

Keywords: Carbone complexes; carbido complexes; transition metal complexes; chemical bonding

1. Introduction

Transition metal compounds with metal-carbon bonds are the backbone of organometallic chemistry. Molecules with M-C single bonds are already known since 1849 when Frankland reported the accidental synthesis of diethylzinc while attempting to prepare free ethyl radicals [1,2]. Molecules with a [M]=CR_2 double bond (carbene complexes) or a [M]≡CR triple bond (carbyne complexes) were synthesized much later [3-6]. Two types of compounds with metal-carbon double or triple bonds having different types of bonds are generally distinguished, which are named after the people who isolated them first. Fischer-type carbene and carbyne complexes are best described in terms of dative bonds following the Dewar-Chatt-Duncan (DCD) model [7,8] [M]⇆CR_2 and [$M^{(-)}$]⇄$CR^{(+)}$ whereas Schrock-type alkylidenes and alkylidynes are assumed to have electron-sharing double and triple bonds [M]=CR_2 and [M]≡CR [9-11].

This review deals with transition metal complexes with metal-carbon bonds to two types of ligands, which have only recently been isolated and theoretically studied. One type of ligand are carbones CL_2 [12], which are carbon(0) compounds with two dative bonds to a carbon atom in the excited ^{1}D state L→$\underline{\bar{C}}$←L where the carbon atom retains its four valence electrons as two lone pairs that can serve as four-electron donors [13,14]. Thus, carbones CL_2 are four-electron donor ligands whereas carbenes CR_2 are two-electron donors. Carbenes have a formally [15] vacant p(π) orbital that can accept electrons in donor-acceptor complexes M⇆ CR_2 whereas carbones are double (σ and π) donors in complexes [M]⇇CL_2. A good Lewis acid acceptor fragment A for a carbene complex has a vacant σ orbital and an occupied π orbital whereas a suitable acceptor for a carbone is a double Lewis acid with vacant σ and π orbitals as shown in figure 1a and 1b. If the Lewis acid A has an occupied π orbital it would lead to π repulsion with the π lone pair of the carbone CL_2, whereby the repulsive interaction is reduced if L is a good π acceptor (Figure 1c). The two electron lone pairs of a carbone may bind to one or two monodentate Lewis acids A or protons or to a single bidentate Lewis acid as shown in Figure 1. The large second proton affinity is a characteristic feature of carbones, which distinguishes them from carbenes [16]. Examples of all cases are known and are described below.

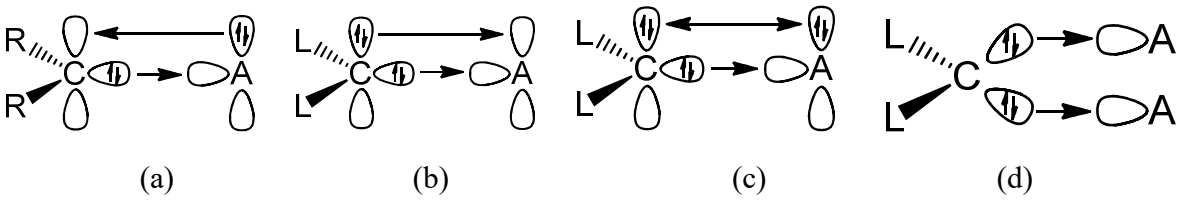

Figure 1. Schematic representation of the most important orbital interactions between carbene ligands CR_2 and carbones CL_2 with Lewis acids A. (a) Carbene complex with a monodentate Lewis acid; (b) Carbone with a bidentate Lewis acid; (c) Carbone with a monodentate Lewis acid; (d) Carbone with two monodentate Lewis acids.

It is important to realize that the two electron lone-pairs of a carbone CL_2 may additionally engage in π-backdonation to the ligands L whose strength depends on the availability of vacant π orbitals of the ligands L. Stronger π acceptor ligands L enhance the π-backdonation L←$\underline{\bar{C}}$→L which leads to wider bending angles at the carbon atom (Figure 2). The significant bending of free $C(CO)_2$ [17,18] can straightforwardly be explained in terms of dative bonding in carbon suboxide C_3O_2 [19,20]. The π-acceptor strength of ligands L thus modulates the donor interaction of the carbone CL_2.

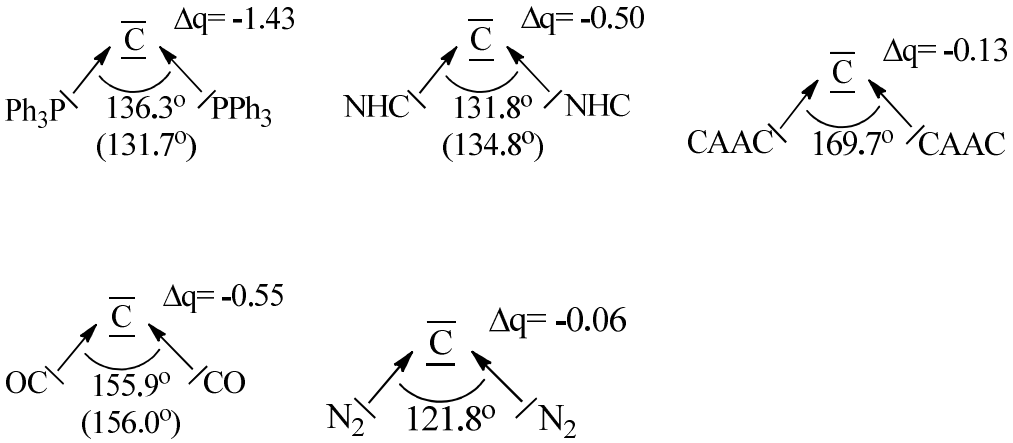

Figure 2. Calculated and (in parentheses) experimental bond angles of carbones CL_2 with different ligands L and partial charges Δq of the central fragments. The data are taken from ref. 20.

The following list gives some essential features of carbones and their differences to carbenes. At the same time we want to stress that the distinction between carbenes and carbones are just a useful classification of compounds, which are a helpful model to explain the structures and reactivity of molecules. Nature does not exhibit a strict distinction line and there are complexes with electronic structures that have intermediate features between both classes of compounds. Carbenes and carbones are two ordering principles like ionic and covalent bonding. Intermediate cases are common and yet, the two concepts are essential ingredients of chemistry. The first part of this review summarizes experimental and theoretical work about transition metal complexes with carbone ligands [M]-CL_2.

1. Carbones are neutral carbon(0) compounds of the general formula CL_2, which possess two electron lone pairs of electrons of σ and π symmetry, respectively.
2. Carbones CL_2 have dative σ bonds L→$\underline{\bar{C}}$←L and weaker π backdonation L←$\underline{\bar{C}}$→L which resemble donor-acceptor bonds in transition metal complexes.
3. The carbon atom of carbones has very large electron densities and thus, unusually large negative partial charges.
4. In contrast to carbenes, carbones exhibit high first and second proton affinities (PAs) in the region of about 290 and 150 - 190 kcal/mole, respectively; the second PA is a sensitive probe for the divalent C(0) character of a CL_2 molecule. Carbones can take up one and two protons with formation of $[HCL_2]^+$ cations or $[H_2CL_2]^{2+}$ dications, respectively.
5. Carbones have a bent equilibrium geometry where the bending angle becomes wider when the ligand L is a better π acceptor.
6. Carbones can take up one or two monodentate Lewis acids A building the complexes A←$C(L_2)$ and A←$C(L_2)$→A or one bidentate Lewis acid A⇇$C(L_2)$.

The second type of transition metal complexes with a carbon ligand features species with a naked neutral carbon atom as a ligand [M]-C, which can be considered as endpoint of the series [M]-CR_3 → [M]-CR_2 → [M]-CR → [M]-C. Complexes with negatively charged carbon ligands [M]-C^-, which are isoelectronic to nitride complexes [M]-N and are termed as carbides, were synthesized in 1997 by Cummins [21]. The first neutral carbon

complex [M]-C, which was prepared and structurally characterized was reported in 2002 by by Heppert and co-workers [22]. They isolated the diamagnetic 16 valence electron ruthenium complexes [(PCy_3)$LCl_2Ru(C)$] (L= PCy and 1,3-dimesityl-4,5-dihydroimidazol-2-ylidene; Cy = Cyclohexyl) by a metathesis facilitated reaction. Quantum chemical calculations of model compounds suggested that the Ru-C bond in the complexes is best described by an electron-sharing double bond like in Schrock carbenes, which is reinforced by a donor bond [Ru]⇇C| [23]. The field of neutral carbon complexes was systematically explored in recent years by Bendix [24]. This review summarizes in its second part the research in transition metal complexes with a naked carbon atom as ligand [M]-C that has been accomplished since 2002.

2. Transition metal complexes with carbone ligands [M]-CL_2

2.1. Transition metal addition compounds of symmetrical carbones $C(PR_3)_2$

Among the existing carbones with a symmetric P-C-P skeleton, five species (**1a** to **1e**) are known today as donor ligands to various transition metal fragments as outlined in Figure 3. From other linear or bent carbones with this skeleton, no transition metal complexes are described so far.

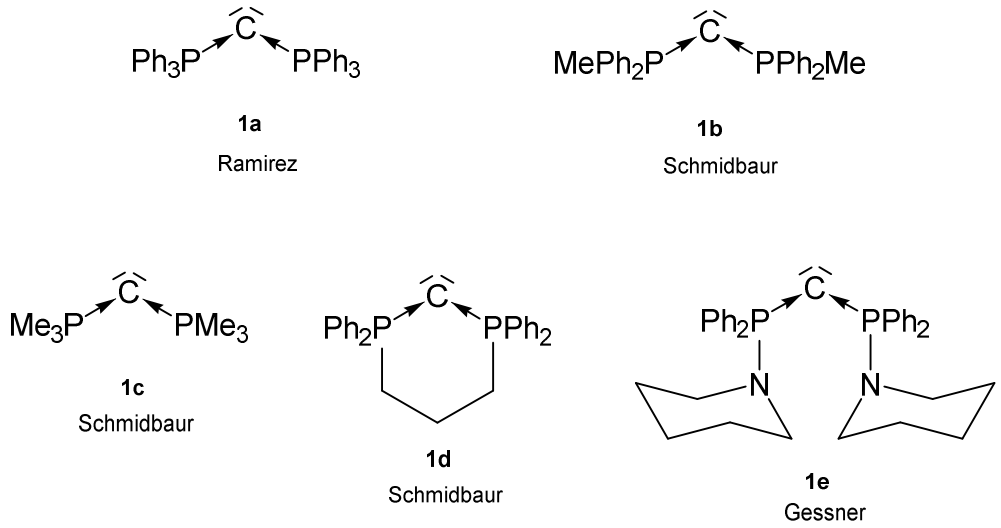

Figure 3. Symmetric carbones **1a** – **1e** as ligands for transition metal complexes.

1a was detected by Ramirez in 1961 [25] and **1b** - **1d** stem from the laboratory of Schmidbaurs group [26]. Later on a series of related carbones were synthesized, but for which transition metal complexes are unknown so far. Quite recently the new amino substituted carbone **1e** was published together with Zn and Rh addition compounds [27]. In the ^{31}P NMR spectra singlets at about -4.50 ppm (**1a**), -6,70 (**1b**), -29.6 (**1c**) -22.45 (**1d**), and 12.5 pm (**1e**) confirm the symmetric array of the compounds. All carbones have a bent structure but a linear form of **1a** is realized if crystallized from benzene [28]. **1a** has a short P-C distance of 1.633(4) Å and the P-C-P angle amounts to 130.1(6)º [29]. The carbone **1b** exhibits a slightly longer P-C distance of 1.648(4) Å and the introduction of two less bulky methyl groups allows a more acute P-C-P angle of 121.8(3)º [30]. **1d** has similar P-C bond distances of 1.645(12) Å 1.653(14) Å and the shortest P-C-P angle in this series of 116.7(7)º [31,32]. For **1c**, gas phase electron diffraction studies result in a P-C distance of 1.594(3) Å and a P-C-P angle of 147.6(5)º assuming an apparent non-linearity but linearity in the average structure [31]. All structural parameters of **1e** are close to those of **1a** (P-C = 1.632(2) Å, P-C-P angle = 136.5(3)º [27].

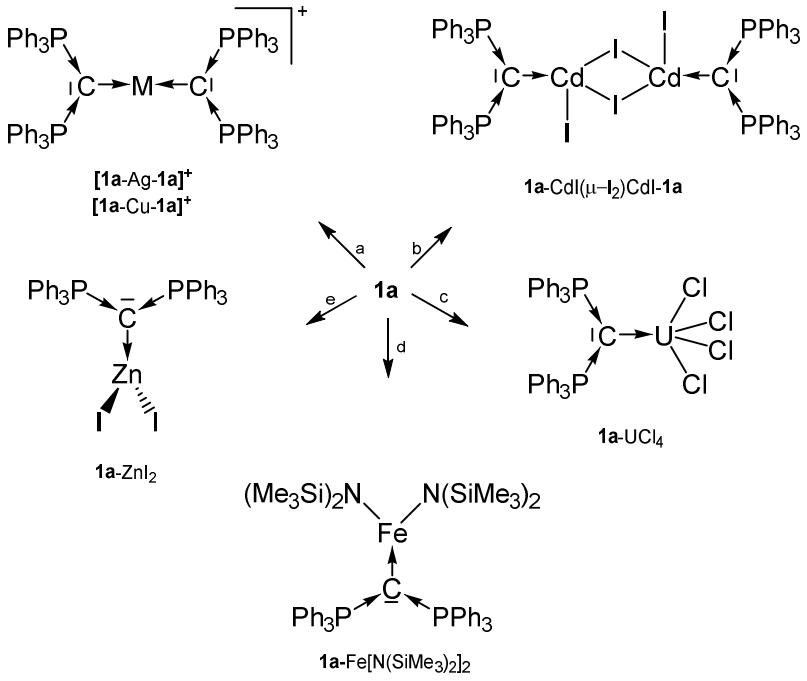

Scheme 1: Selected transition metal compounds with the carbone **1a** as two electron donor ligand; a) MI, b) CdI_2, c) UCl_4, d) $Fe(N\{SiMe_3\}_2)_2$, e) ZnI_2.

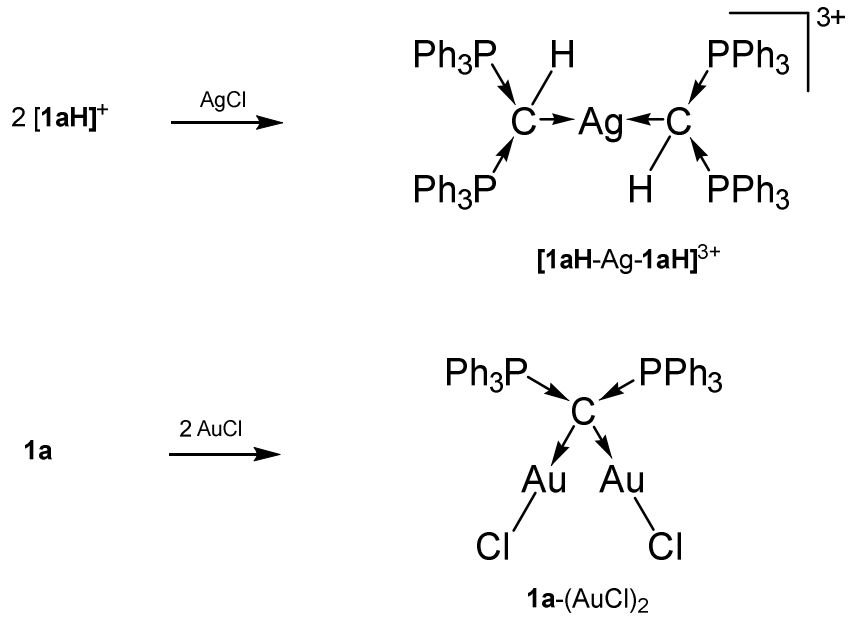

Scheme 2: Selected transition metal compounds with the carbone **1a** as four electron donor ligand.

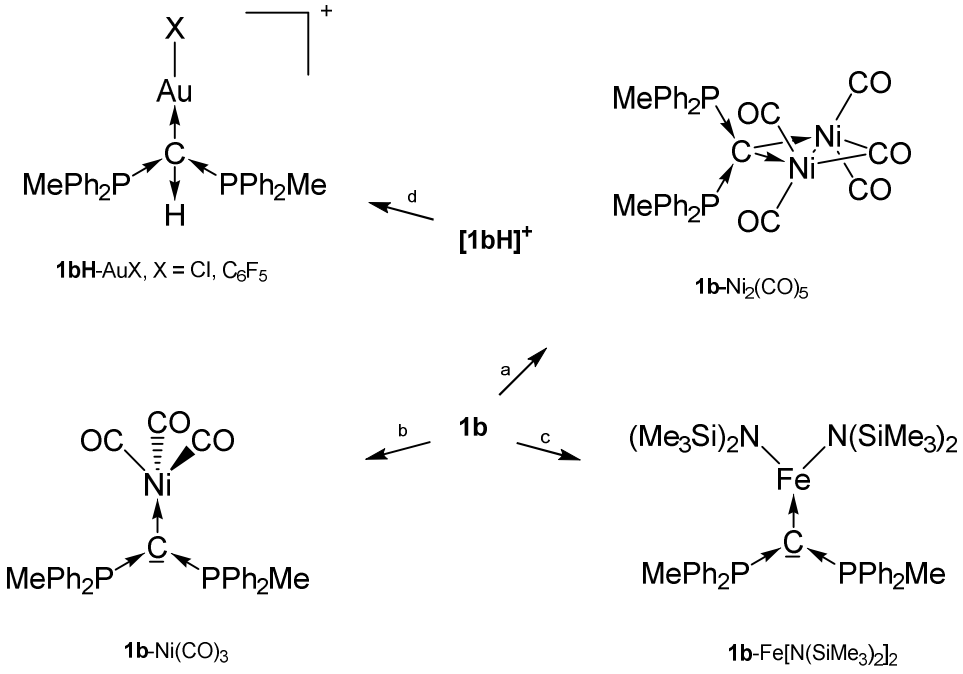

Scheme 3: Selected transition metal complexes with the carbone **1b** as two and four electron donor ligand. a) $Ni(CO)_4$, b) $Ni(CO)_4$ under CO atm, c) $Fe(N\{SiMe_3\}_2)_2$, d) AuX(tht).

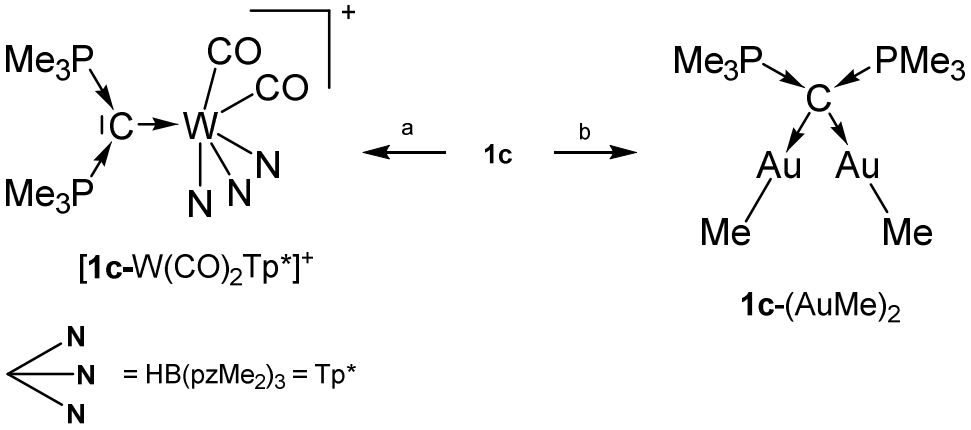

Scheme 4: Transition metal complex with the carbone **1c** as two and four electron donor ligand. a) $[Tp^*(CO)_2W{\equiv}CPMe_3]^+/PMe_3$, b) 1c/ 2 $MeAuPMe_3$.

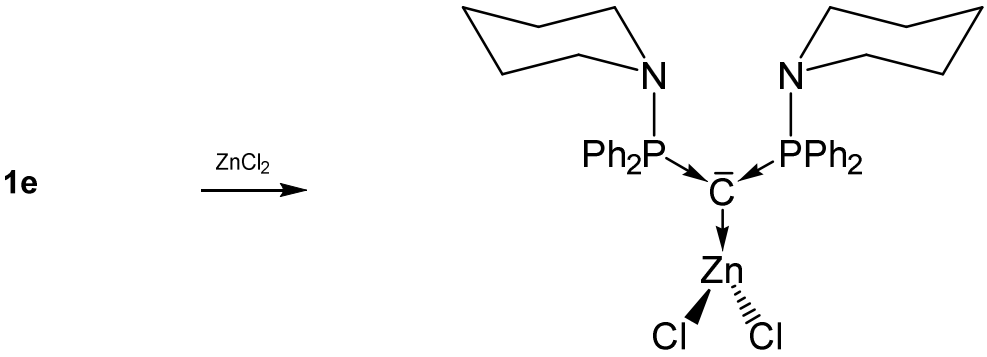

Scheme 5: Selected transition metal complex with the carbone **1e** as two electron donor ligand.

In Table 1 transition metal addition compounds between carbones with the P-C-P core are collected. All compounds show longer P-C bonds than the basic carbones as consequence of the competition of the occupied p orbital at C(0) between the two P-σ* orbitals and those of A.

Occupied d orbitals of Ni in the **1a**-$Ni(CO)_3$ complex elongate the C-Ni bond to a carbone (2.110 Å) [36] but leads to relative short bond length to a NHC (1.971 Å) moiety [33]. In contrast, UCl_4 leads to a short bond to a carbone (2.411 Å) [48] indicating an appreciable U-C double bond character and a long one to a NHC base (2.612 Å) [34,35].

Table 1. Transition metal complexes with the carbones **1a** to **1e** including C-M and P-C bond lengths and P-C-P angles and ^{31}PNMR shifts in ppm.

Nr.	^{31}P NMR	C-M	P-C	P-C-P	Ref
Transition metal complexes with the carbone **1a**					
1a→$Ni(CO)_2$	19.20	1.990(3)	1.677(3) 1.676(3)	132.13(16)	[36]
1a→$Ni(CO)_3$	9.92	2.110(3)	1.681(3) 1.674(3)	124.58(19)	[36]
1a→ZnI_2	17.8	2.000(9)	1.691(9) 1.703(8)	128.3(6)	[37]
1a→CdI(μ I_2)CdI←**1a**	18.5	2.25(1)	1.700(9) 1.68(1)	124.8(7)	[37]
[**1a**→Hg←**1a**][Hg_2Cl_6]	21.2	2.057(6) 2.082(7)	1.731(6) 1.706(6) 1.737(6) 1.702(7)	124.2(4) 125.7(3)	[38]
[**1a**→Ag←**1a**]I	13.6	2.115(8) 2.134(7)	1.656(7) 1.690(7) 1.667(7) 1.663(7)	128.5(5) 129.1(5)	[39]
[**1a**→Cu←**1a**]I	15.8	1.944(5) 1.951(5)	1.683(6) 1.688(6) 1.673(6) 1.694(5)	125.6(3) 128.3(3)	[38]
[**1a**→ReO_3][ReO_4]	29.5	1.997(7)	1.771(8)	123.1(4)	[40]
1a-CuCl	16.5	1.906(2)	nr	123.8(1)	[41]
1a→Cu-C_5H_5	8.5	nr	nr	nr	[42]
1a→Cu-C_5Me_5	7.5	1.922(6)	1.668(5) 1.660(6)	136.0(4)	[42]
1a→$CuPPh_3$	3.7	nr	nr	nr	[42]
1a→AgCl	16.5	nr	nr	nr	[41]
1a→AgCp*	6.5	nr	nr	nr	[42]
1a→Au-C≡C-R	nr	2.082(2)	1.688(2) 1.682(2)	133.64(13)	[43]
R = $C_6H_4NO_2$-p					
1a→Au-$CH(COMe)_2$	nr	nr	nr	nr	[43]
1a→AuCl	13.7 14.4	nr	nr	nr	[41]
[1a→Ir(COD)]PF_6	nr	nr	nr	nr	[44]
1a→VCl_3	21.13	2.050(3)	1.712(2), 1.722(2)	123.6(2)	[45]
1a→FeCl(μCl_2)FeCl←**1a**	par	2.043(7)	1.689(7) 1.712(7)	121.3(4)	[46]
1a→Fe[$N(SiMe_3)_2$]$_2$	par	2.147(2)	1.702(2) 1.720(2)	120.0(1)	[47]
1a→$FeCl_2$	par	2.055(8)	1.709(7) 1.702(7)	122.7(5)	[46]
1a→Fe(CH_2Ph)$_2$	par	2.097(5)	1.694(5) 1.671(5)	124.5(3)	[46]

1a→FeCl[N(TMS)$_2$]	par	nr	nr	nr	[46]
1a→FeOTf[N(TMS)$_2$]	par	2.040(3)	1.701(3) 1.704(3)	122.1(2)	[46]
1a→UCl_4	nr	2.411(3)	1.705(3) 1.719(3)	125.05(16)	[48]
1a→$(AuCl)_2$	21.2	2.078(3) 2.074(3)	1.776(3) 1.776(3)	117.30(15)	[43]
[1aH-Ag-**1a**H]$^{3+}$	23.6	2.221(5)	1.770(7) 1.779(7)	119.9(4)	[49]
[1aH-Au-**1a**H]$^{3+}$	26.1	nr	nr	nr	[43]
[1aH→AuCl]$^+$	22.1	nr	nr	nr	[43]
Transition metal complexes with the carbone **1b**					
1b→Fe[N(SiMe$_3$)$_2$]$_2$	par	2.100(2)	1.694(2) 1.696(1)	120.8(9)	[47]
1b→$Ni(CO)_3$	2.6	2.091(2)	1.683(2) 1.673(2)	122.3(1)	[50]
1b→$Ni_2(CO)_5$	12.1	2.080(5) 2.070(5)	1.742(5) 1.743(5)	117.1(3)	[50]
[1bH→AuC$_6$F$_5$]+	22.7	2.029(6)	1.781(2) 1.792(2)	119.1	[51]
[1bH→AuCl]+	22.1	nr	nr	nr	[51]
Transition metal complexes with the carbone **1c**					
[1c→W(CO)$_2$(Tp*)]PF$_6$	36	2.11(1)	1.75(2) 1.77(1)	114.5(8)	[52]
1c→$(AuMe)_2$	nr	nr	nr	nr	[124]
Transition metal complexes with the carbone **1d**					
1d→$Ni(CO)_3$	3.5	2.0661(9)	1.712(2) 1,722(2)	117.19(9)	[45]
Transition metal complexes with the carbone **1e**					
1e-$ZnCl_2$	28.9	1.994(2)	1.686(2)	125.3(1)	[27]
1e-Rh(CO)(acac)	32.9	2.092(3)	1.685(3)	128.56(17)	[27]

The cation [**1a**-ReO_3]$^+$ holds the longest one with 1.771(8) Å indicating an appreciable C=Re double bond character. This feature applies also in part to **1a**-UCl_4 and **1c**-W(CO)$_2$N$_3$ with elongated P-C bonds; a partial C-U double bond is confirmed by theoretical calculations. Similar long P-C bonds are found in the trication [**1a**H-Ag-**1a**H]$^{3+}$, in **1a**-$(AuCl)_2$, and in **1b**-$Ni_2(CO)_5$, where the carbone provides each two electrons to two accepting Lewis acids as depicted in Figure 1d. The P-C-P angles are in the range between 115º and 132º reflecting the

required space of the appropriate Lewis acid. The ^{31}P NMR shift of the carbone **1a** amounts to about -5 ppm and those of the related addition compounds are shifted to lower fields and range between 4 ppm and 30 ppm. All iron(II) complexes of **1a** and **1b** are paramagnetic and ^{31}P NMR spectra could not be obtained.

For the ^{31}P NMR spectrum of the carbone **1b**, a shift of -6.70 ppm was recorded [26]. With exception of **1b**→$Ni(CO)_3$ which resonate at 2.6 ppm, low field shifts between 12 and 22 ppm were found when **1b** act as a four electron donor [50].

1e-$ZnCl_2$ [27] and **1a**-ZnI_2 [37] have closely related structural parameters but exhibit shorter C-Zn bond lengths than to related NHC-addition compounds (Δ = 0.051 Å) [53]. In both compounds a nearly perpendicular array of the ZnX_2 and the PCP plane are found. No tendency for an additional N-coordination to the amino ligand of **1e** is recorded for the $ZnCl_2$ addition compound. In contrast the Rh-C distances in **1e**-$Rh(CO)_2$(acac) are longer (Δ = 0.117 Å) than in the corresponding NHC compound [54] and a partial π interaction was found by DFT calculation; Rh shows also no tendency for coordination of the adjacent amino groups [27].

2.2. Transition metal addition compounds of carbones $C(PR_3)_2$ with an additional pincer function

Starting material for **2a** is not the free carbone Ph_2P-CH_2-PPh_2-C-PPh_2-CH_2-PPh_2 which could not be prepared so far, but the dication $[Ph_2P$-CH_2-PPh_2-CH_2-PPh_2-CH_2-$PPh_2]^{2+}$ as reported by Peringer [55]; the basic pincer ligand **2b** was presented by the group of Sundermeyer in 2019 and the ^{31}P NMR shift δ = -5.6 ppm. The P-C-P angle in **2b** amounts to 133.76(13)° , P-C = 1.633(2), 1.642(2) [56].

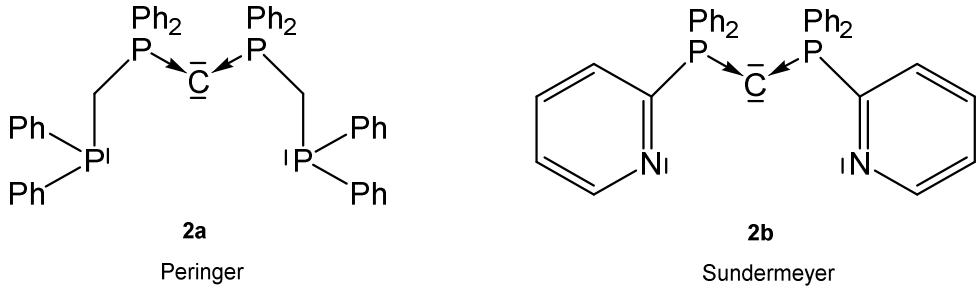

Figure 4. Tripodal basic pincer ligand **2a** and **2b**.

Table 2. Transition metal complexes with the phosphine based pincer ligands **2a** and the pyridyl based pincer ligand **2b**; C-M and P-C distances are included and ^{31}P NMR shifts in ppm.

Nr.	^{31}P NMR	C-M	P-C	P-C-P	Ref
Transition metal complexes with the tripodal carbone **2a**					
[2a(PdCl)]Cl	34.5	2.062(2)	1.694(3)	124.9(2)	[55,57]
[2a(NiCl)]Cl	36.4	1.942(4)	1.6925(18)	125.1(2)	[57]
[2a(NiCl)]$NiCl_4$	nr	1.930(7)	1.696(7)	126.3(4)	[57]
			1.701(7)		
[2a(PtCl)]Cl	35.7	2.060(4)	1.692(5)	124.86(15)	[57]
[2a(NiMe)][$AlCl_2Me_2$]	31.8	1.959	1.697	120.9	[58]
[**2a**(AuCl)]TfO_2		2.080(8)	1.723(8)	124.5(5)	[59]
[**2a**(AuCl)]$(NO_3)_2$	40.8	2.060(3)	1.721(3)	125.1(2)	[59]
[2a(AuI)]$(TfO)_2$	41.1	2.082(8)	1.723(8)	124.9(5)	[59]
[2aH-PdCl]$^{2+}$	**[**42.4	2.102(3)	1.803(3)	121.9(2)	[55]
[2aH-PtCl]$^{2+}$	44.4	2.106(4)	1.811(4)	120.4(2)	[57]
			1.823(4)		
[2aH-NiCl]$^{2+}$	32.7	1.990	1.801 – 1.834	121.1	[57,58]
Transition metal complexes with the tripodal carbone **2b**					
2b($CeBr_3$THF)	-10.2	2.597(6)	1.672(6)	122.5(4)	[60]
2b(CeBr)**2b**	nr	2.573(6)	1.684(7)	120.5(4)	[60]
		2.597(6)			
2b(UCl_4)	nr	2.471(7)	1.696(7)	121.3(4)	[48]
2b($TiCl_3$) [57]	18.24	2.144(6)	1.670(3)	129.9(4)	[56]
			1.670(3)		
2b($Cr(CO)_3$)	6.97	2.212(2)	1.651(3)	133.6(2)	[56]
			1.650(3)		
2b($MnCl_2$)	par	2.1843(14)	1.6671(17)	127.70(9)	[56]
			1.6636(17)		
2b($CoCl_2$)	par	2.015(6)	1.680(7)	127.5(3)	[56]
			1.661(7)		
2b($Mo_2(CO)_7$)	9.49	2.355(4)	1.722(4)	120.4(2)	[56]
			1.724(4)		
[**2b**(PdCl)]Cl	31.6	2.004(4)	1.689(4)	132.4	[56]
			1.676(4)		
2b-$Ni_2(CO)_4$	34.20	2.0635(18)	1.7142(18)		[56]
		2.0912(18)	1.7146(18)		

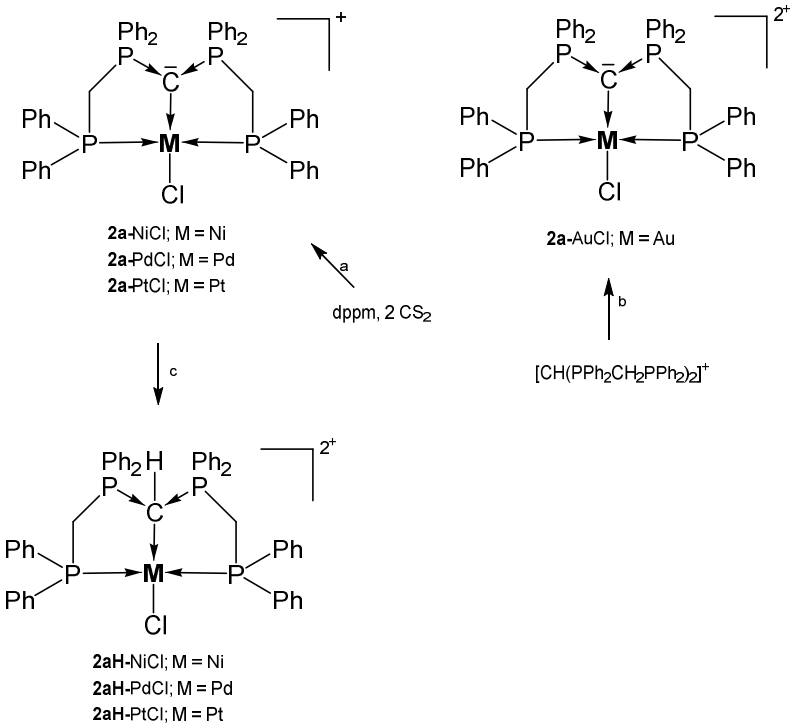

Scheme 6. Selected compounds with the pincer ligands **2a** and **2aH.** a) MCl_2 with a mixture of dppm and 2 eq. of CS_2, b) AuCl(tht)/HNO_3, c) HCl.

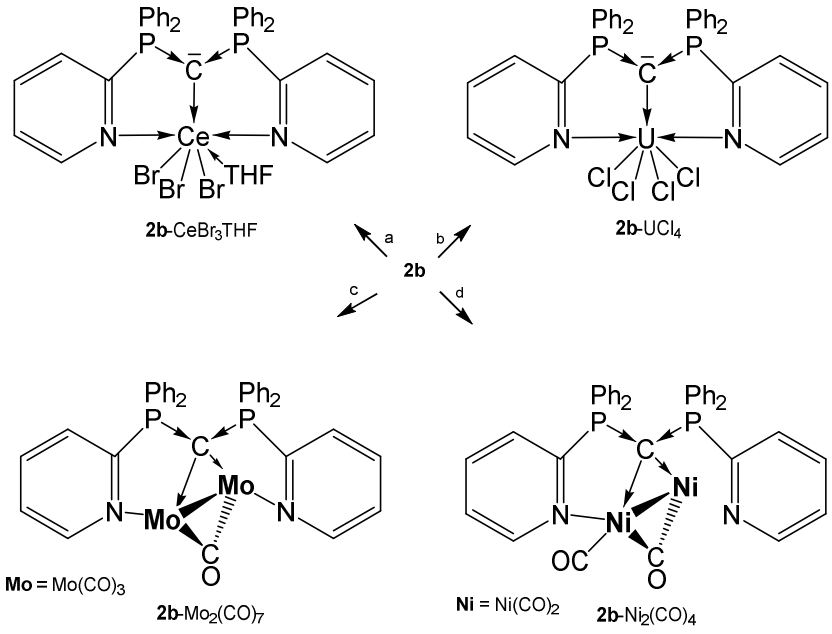

Scheme 7. Selected compounds with the pincer ligand **2b** as two and four electron donor. a) $CeBr_3$ in THF, b) UCl_4, c) 2 eq $Mo(CO)_3(NCMe)_3$, d) 2 eq $Ni(CO)_4$.

Various cationic complexes where reported with the pincer ligand **2a** and group 10 metal halides and one dication with the group 11 metal Au. The ^{31}P NMR shifts range between 32 and 41 ppm. As with **1a** the carbone carbon atom of **2a** is basic enough to accept a proton to generate complexes of the type **2aH**-MCl dications with all group 10 elements.

A series of complexes with the N,C,N pincer ligand *sym*-bis(2-pyridyl)tetraphenylcarbodiphosphorane (**2b**) were reported recently by the group of Sundermeyer. Remarkable is the molybdenum complex **2b**-$Mo_2(CO)_7$ in which **2b** provides four pairs of electrons for donation to a Mo_2 unit with an Mo-Mo separation of 3.0456(5) Å [56].

2.3. Transition metal addition compounds of Carbones $C(PR_3)_2$ with an additional ortho metallated pincer function

Source for the Rh complex **3a**-$Rh(PMe_3)_2H$ was the half pincer compound **5a**-$Rh(C_6H_8)$ upon reacting with PMe_3 under loss of cod. **3a**-$Pt(SMe_2)$ forms upon reacting **1a** with $[Me_2Pt(SMe_2)]_2$ and loss of 4 molecules of CH_4 [61]. PEt_3 replaces the labile bonded SMe_2 group of **3a**-$Pt(SMe_2)$ to produce **3a**-$PtEt_3$, which is transformed with $P(OPh)_3$ into **3a**-$Pt(OPh)_3$. The dication [**3a**-$PtPEt_3(\mu$-$Ag_2)Et_3PPt$-**3a**]$^{2+}$ was obtained upon addition of AgOTf to **3a**-$PtPEt_3$. According to the carbone C atom as four electron donor the Pt complexes with μ-Ag functions show long Pt-C distances between 1.737 and 1.749 Å (mean values) and the ^{31}PNMR shifts are in the narrow range of 33 and 36 ppm [63]. More complicated is the formation of **3a**-Pt(CO); it stems from hydrolysis of the related **3a**-$Pt(CCl_2)$ complex (not isolated) [62].

The carbone complex **3b**-Pt(CO) was obtained from reacting the yldiide platinum complex (see **Scheme 9**) with 1 atm CO that inserts into the N-Si bond of the yldiide.

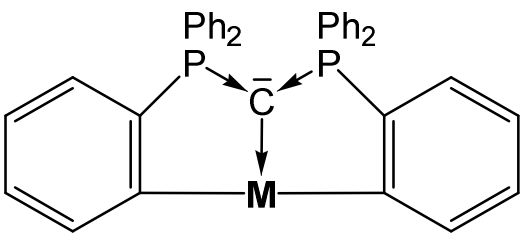

3a

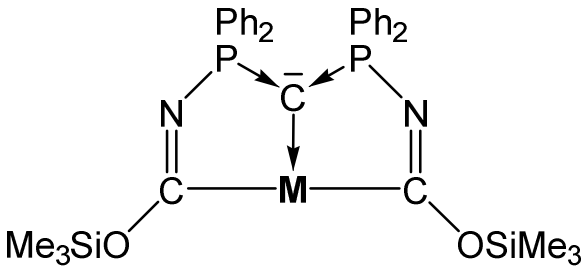

3b

Figure 5. Bis-ortho metallated pincer complexes **3a** and **3b**.

Table 3. Transition metal complexes with ortho metallated tripodal pincer ligand **3a** derived from **1a** and the related pincer ligand **3b** and ^{31}P NMR shifts.

Nr.	^{31}P NMR	C-M	P-C	P-C-P	Ref
Transition metal complexes with the tripodal ligand **3a**					
3a-Rh(PMe$_3$)$_2$H	8.56	2.203(3)	1.674(3)	138.32(18)	[61]
3a-PtSMe$_2$	30.42	nr	nr	nr	[61]
3a-PtCO	41.5	2.037(5)	1.706(3)	128.4(3)	[62]
3a-PtPEt$_3$	28.5	2.067(2)	1.697(2)	124.88(14)	[63]
3a-PtP(OPh)$_3$	nr	nr	nr	nr	[63]
[**3a**-PtPEt$_3$(μ-AgPPh$_3$)$_3$]$^+$	32.5	2.130(4)	1.737	126.0(2)	[63]
[**3a**-PtP(OPh)$_3$ (μ-AgPEt$_3$]$^+$	36.0	2.105(3)	1.743	122.9(2)	[63]
[**3a**-PtPEt$_3$(μ-Ag$_2$)Et$_3$PPt-**3a**]$^{2+}$	33.4	2.128(3)	1.749	125.29(18)	[63]
3aH-PtCl	27.9	2.077(6)	1.796(6)	123.4(4)	[62]
Transition metal complexes with the tripodal ligand **3b**					
3b-Pt(CO)	46.9	2.002(5)	nr	133.3(3)	[64]

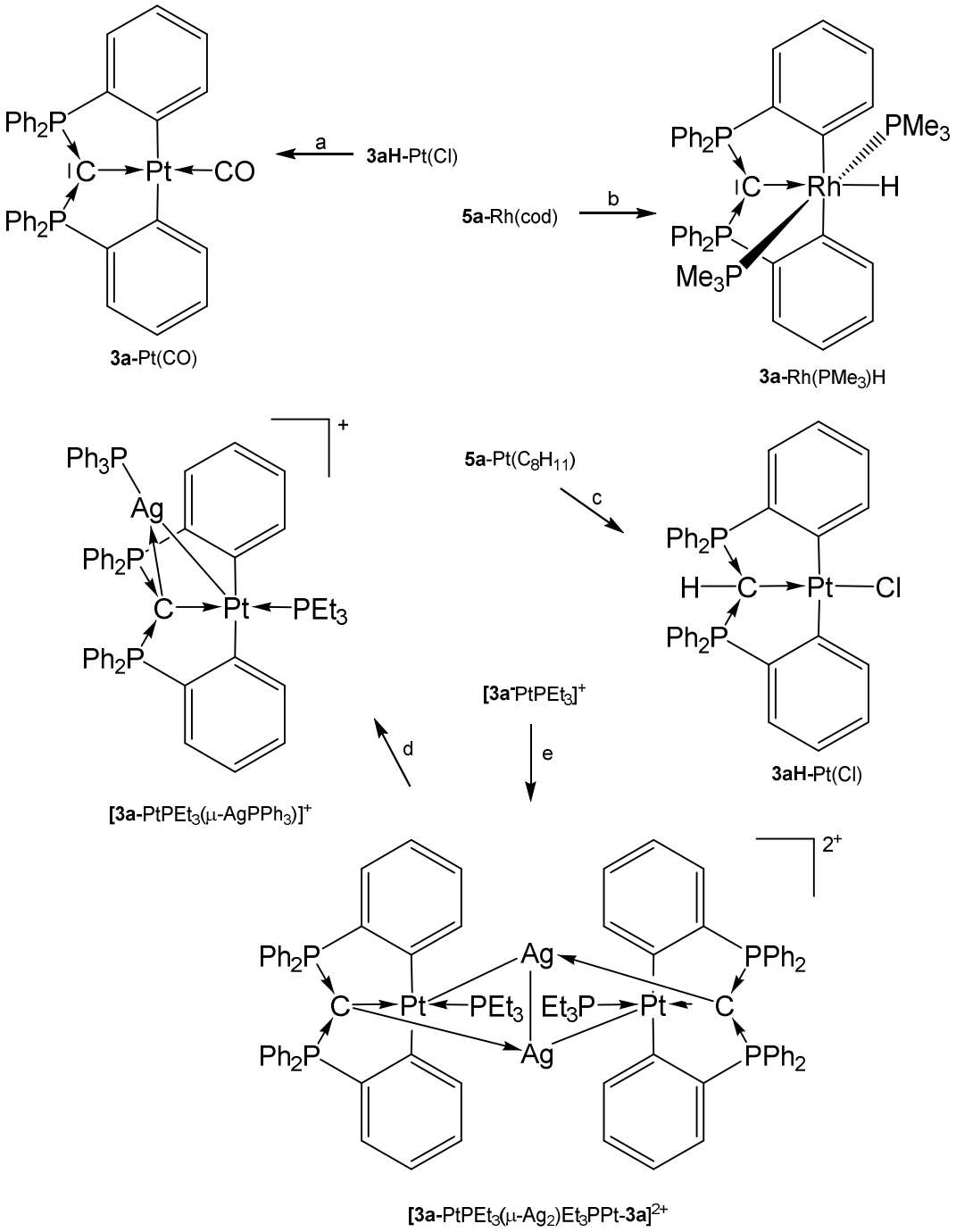

Scheme 8. Selected addition compounds with the pincer ligand **3a** and **3aH** and those with the Ag-bridged cations or dication, respectively. a) from **3aH**-PtCl via **3a**-Pt(CCl_2) and H_2O, b) PMe_3, c) from **5a**-Pt(C_8H_{11}) (see **Scheme 11**) and $CHCl_3$, d) PPh_3, e) 2 AgOTf.

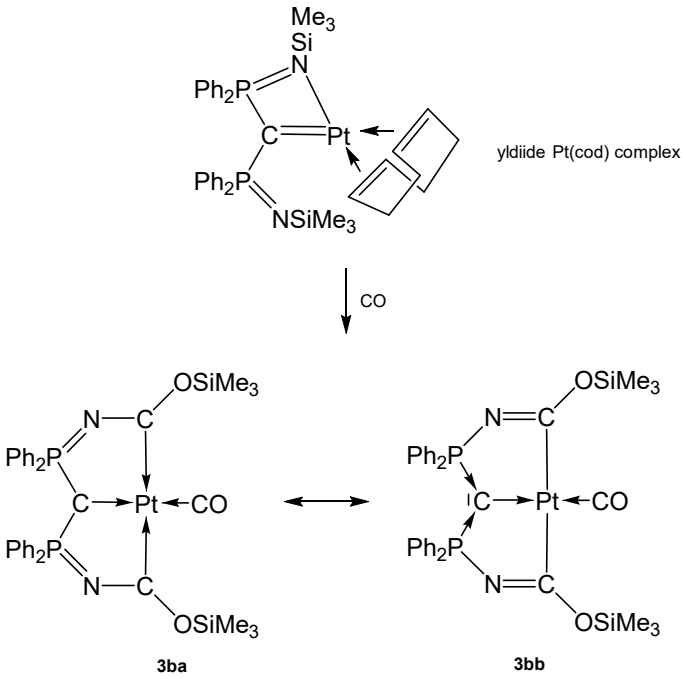

Scheme 9. Two mesomeric forms of **3b**-Pt(CO); **3ba** favors a tricarbene coordination at Pt(0) whereas **3bb** is consistent Pt(II) forming two C-Pt s-bonds similar to **3a**-Pt(CO). The short central C-Pt bond length of 2.002 Å indicates a partial doubly donation of the carbone C atom as shown in Figure x1b. The planar environment at Pt is typical for Pt(II) and supports this view [64].

2.4. Transition metal complexes with p-c-p five membered ring

The carbone **4** was obtained by deprotonation of the cation [**4H**]$^+$. According to two P atoms in different chemical environments two doublets in the ^{31}P NMR spectrum were recorded at δ = 60.0 and 71.5 ppm; $^2J_{PP}$ = 153 Hz. From X-ray determination stem the P-C(1) and P-C(2) distances of 1.644(19) and 1.657(17) Å, respectively, and the P-C-P angle amounts to 104.82(10)º [65]. The bond lengths are close to that reported for the carbone **1a.**

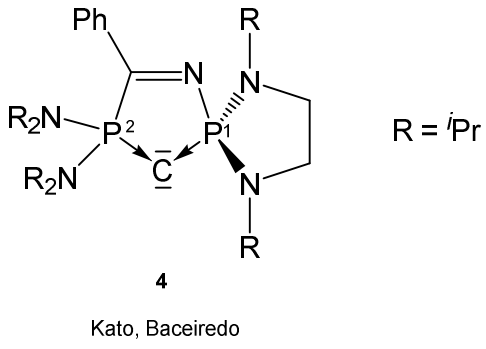

Figure 6. Structure of compound **4.**

Table 4. Transition metal complexes with the cyclic carbone **4**, containing ^{31}P NMR shifts and relevant structural parameters.

Nr.	^{31}P NMR		M-C	P^1-C P^2-C	P-C-P	Ref
4-PdCl(π-C_3H_5)	61.2	71.9 (225)	2.120(2)	1.673(2) 1.694(2)	106.66(13)	[65]
4-RhCl(nbd)	64.6	75.7 (230)	2.115(18)	1.676(18) 1.702(18)	106.86(10)	[65]
4-Rh(CO)$_2$Cl	68.2	75.6 (224)	nr	nr	nr	[65]
4-AuOBu^t	64.1	60.4 (225)	2.018(6)	1.674(7) 1.687(7)	108.5(4)	[66]
4-CuOBu^t	69.8	62.6 (195)	1.8923(15)	1.6763(15) 1.6887(15)	106.90(8)	[66]
4-CuCl	63.2	70.6 (186)	1.8914(19)	1.6700(19) 1.6869(19)	107.20(11)	[66]

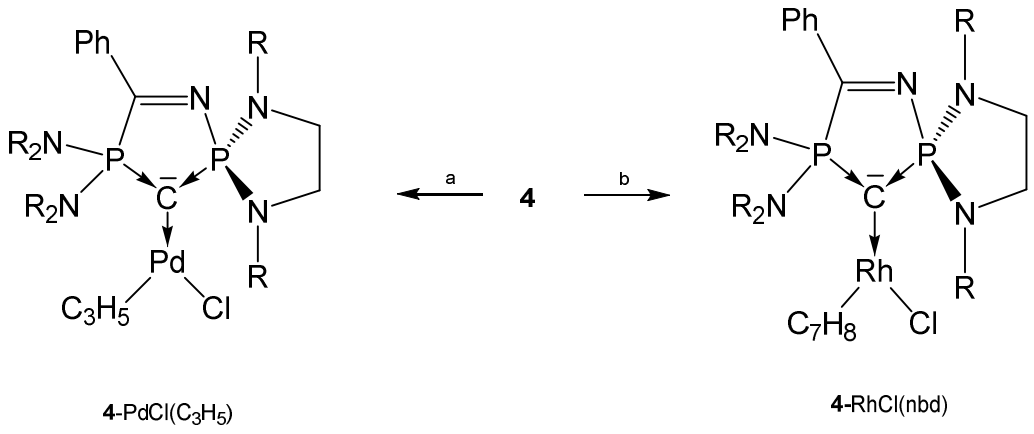

4-PdCl(C_3H_5) **4**-RhCl(nbd)

Scheme 10: Selected complexes with the cyclic carbone **4**. R = *i*Pr. a) [{PdCl(allyl)}$_2$], b) [{RhCl(nbd)}$_2$].

From the cyclic and asymmetric carbone **4** six transition metal complexes are known in which the ligand acts as two electron donor via the C atom. As in the starting compound **4** the P^2-C bond distances are slightly longer than P^1-C ones. Addition of CuCl and AuCl(SMe$_2$) to

4H^+/*t*BuOK generates the compounds **4**-CuO*t*Bu and **4**-AuO*t*Bu, respectively; in CH_3Cl_2 or $CHCl_3$ **4**-CuO*t*Bu is converted into **4**-CuCl [66]. **4**-$Rh(CO)_2Cl$ stems from the reaction of **4** with $[\{RhCl(CO)_2\}_2]$ [65]. **4**-CuO*t*Bu and **4**-AuO*t*Bu catalyze the hydroamination or hydroalkoxylation of alcrylonitrile [66].

2.5. Transition metal complexes with asymmetric P-C-P ligands

Several asymmetric carbones with orthometallation (**5a-M**, **5d-M**), with an additional donor function (**5c**), or with a functionalized phenyl ring (**5b**) were reported that form TM complexes.

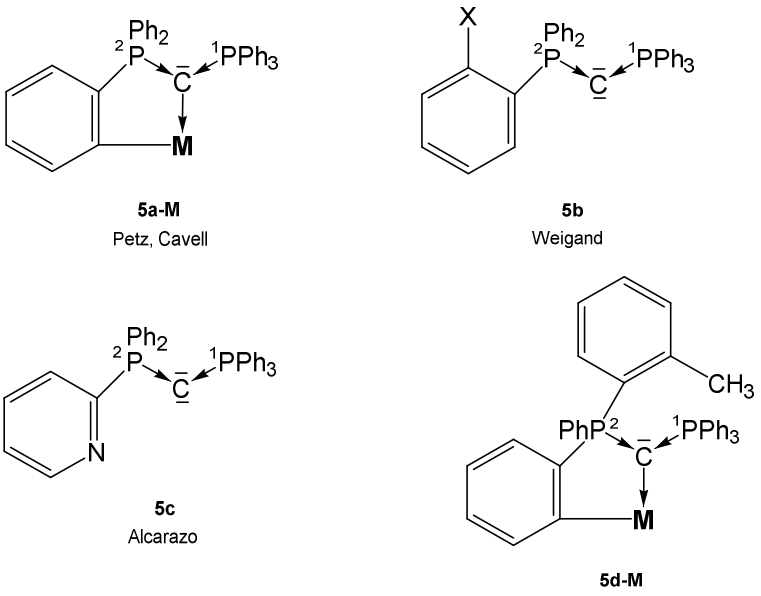

Figure 7. Structures of compounds **5a-M**, **5b**, **5c** and **5d-M**.

The neutral asymmetric carbone **5b** (X = PPh_2) has the structural parameters P^1-C = 1.642(2), P^2-C = 1.636(1) Å, and a P-C-P angle of 140.74(8)º; the P atoms resonate at δ = -6.9 and -3.4 ppm ($^2J_{PP}$ = 93 Hz) [67]. Those of **5c** are P^1-C = 1.6416(16) Å, P^2-C = 1.6398(17) Å, and P-C-P = 133.25(10)º [68]. Three complexes in which the carbone **1a** is half-side orthometallated forming **5a-M** complexes are described [61,65,69].

Table 5. Transition metal complexes with the unsymmetrical carbones **5a – 5d**; ^{31}P NMR shifts in ppm.

Nr	^{31}P NMR ($^{2}J_{PP}$)	M-C	P^1-C P^2-C	P-C-P	Ref.
	Transition metal complexes of **5a-M**				
5a-Ptcod(C_8H_{11})	14.9 5.7 (59.8)	2.072(3)	1.694(4) 1.716(4)	114.8(2)	[69]
5a-Rhcod(p)	10.15 12.40 (50.9)	2.165(2)	1.693(2) 1.692(2)	124.50(13)	[61]
5a-PdC_3H_5	39.8 9.9 (54)	nr	nr	nr	[65]
	Transition metal complexes with the carbone **5b**				
5b-AuCl (X=PPh_2)	8.6 18.7 (52)	2.043	1.701(4) 1.696(2)	126.0(2)	[67]
5b-AuCl (X=PPh_2-AuCl)	25.6 20.2 (47)	2.037(3)	1.690(3) 1.689(3)	131.4(2)	[67]
5b-$(AuCl)_2$ (X=PPh_2-AuCl)	25.4 26.9	2.089 2.064	1.774(5) 1.763(5)	123.6(3)	[67]
5b-$PtMe_2$ (X = Me)	19.3	nr	nr	nr	[70]
	Transition metal complexes with the carbone **5c**				
5c-UCl_4	par	2.461(5)	1.699(5) 1.711(5)	120.6(3)	[48]
[5c$AuPPh_3]^+$	19.70 15.03 (30.7)	2.067(9)	1.688(9) 1.707(9)	124.3(5)	[68]
[5c(CuCl)$(AuPPh_3)]^+$	39.7 26.2 (m)	2.111(4) Au 1.981(5) Cu	1.732(5) 1.750(5)	120.2(3)	[68]
[5c(AuCl)$(AuPPPh_3)]^+$	35.4 27.5 (m)	2.080(9) Au^2 2.127(8) Au^1	1.756(9)	119.3(5)	[68]
	Transition metal complexes with the carbone **5d**				
5d-Pt-**5d**	19.3	-	-	-	[70]

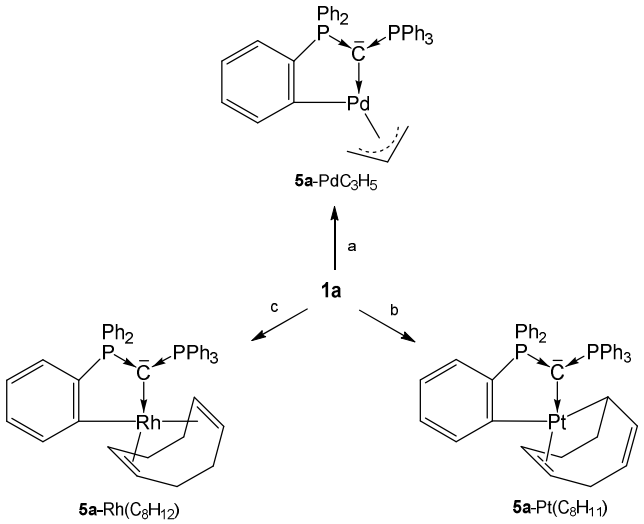

Scheme 11: Selected structures of transition metal complexes with the carbone **5a**; a) ½ [PdCl(allyl); b) 1/3 [PtI_2(cod)]; c) ¼ [RhCl(cod)]. All complexes are formed upon release of the cation [**1aH**]$^+$.

As depicted in Scheme 11, three neutral complexes of **1a** are known in which one of its phenyl group is orthometallated to produce the **5a-M** core. The ^{31}P NMR shift of the unchanged PPh_3 group range between about 6 and 13 ppm whereas for the orthometallated side shifts between 15 and 40 ppm where recorded. Both P-C distances do not differ markedly and amount to about 1.700 Å.

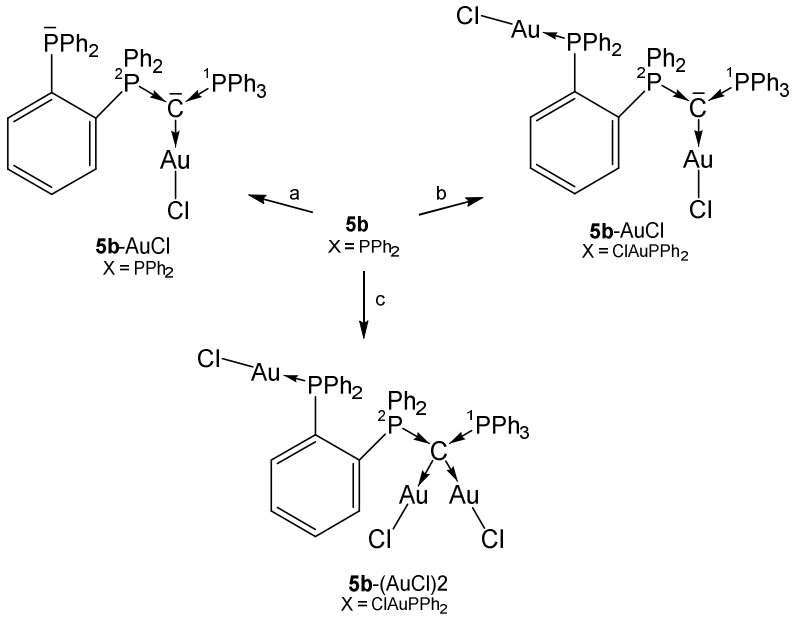

Scheme 12. Selected structures of transition metal complexes with the carbone **5b**. a) [AuCl(tht)], b) 2 [AuCl(tht), 3 [AuCl(tht)].

All complexes shown in Scheme 12 have a further PPh_2 function at the ortho position of one phenyl group of **1a**. In the complex **5b**-$(AuCl)_2$ the carbone provides four electrons for donation with typical long P-C distances of about 1.770 Å [67].

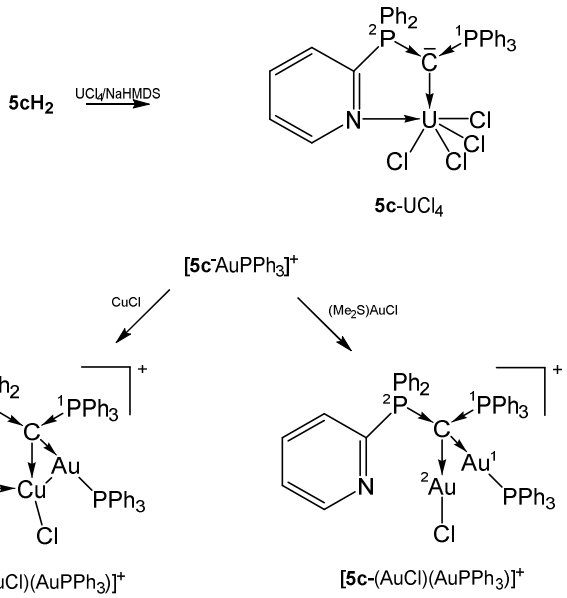

Scheme 13. Selected structures of transition metal complexes with the mono pyridyl substituted carbone **5c.**

The paramagnetic **5c**- UCl_4 exhibits a short C-U distance indicative for a double dative bond of the carbone C atom as in **2b**-UCl_4 and was obtained by reacting UCl_4 with the dication **5c**-H_2/NaHMDS. Upon further coordination of the pyridyl group (U-N = 2.537(4) Å) the U atom attains the coordination number 6 [48].

[5c-$AuPPh_3]^+$ was obtained from reacting the carbone **5c** with $[PPh_3AuCl]/Na[SbCl_6]$. In the cationic complex [**5c**-(CuCl)((AuPPh$_3$)]SbF_6, the carbone **5c** acts as a six electron donor with a Cu-N distance of 2.267(6) Å and Cu-Au separation of 2.8483(10) Å. The Cu and Cl atoms are each disordered over two positions with occupancy of about 0.8 to 0.2. If CuCl is replaced by AuCl as in [**5c**-(AuCl)(AuPPh$_3$)]SbF_6 the C-$AuPPh_3$ distance is slightly elongated and no coordination of the pyridyl N atom is observed. The Au-Au separation is with 3.1274(6) Å too long for a metallophilic interaction. In both compounds, the carbone C atom constitutes a chiral center according to four chemical different substituents and acts as a four electron donor. The PPh_3 group resonates between 15 and 27 ppm [68]. In the related symmetric pyridyl-free

complex **1a**-$(AuCl)_2$ slightly shorter C-Au (2.076(3) Å) were recorded accompanied by longer P-C (1.776(3) Å) bond lengths [43].

2.6. Transition metal complexes of carbones with cyclobutadiene

The carbones **6a** and **6b** can also be seen as an all-carbon four-membered ring bent allene (CBA); **6a** is stable for several hours at -20º but decomposes when warmed up to -5º. The optimized geometry reveals a very acute allene bond angle of 85.0º and coplanarity of the ring carbon atoms including the two nitrogen atoms. The C=C bonds of the allene fragment amount to 1.423 Å and are significantly longer than in typical linear allenes (1.31 Å). Short CN bonds of 1.36 Å indicate some double bond character. The C**C**C carbon atom resonates in the ^{13}C NMR spectrum at 151 ppm. The first and second proton affinities (PAs) are very high amounting to 307 and 152 kcal/mol [71].

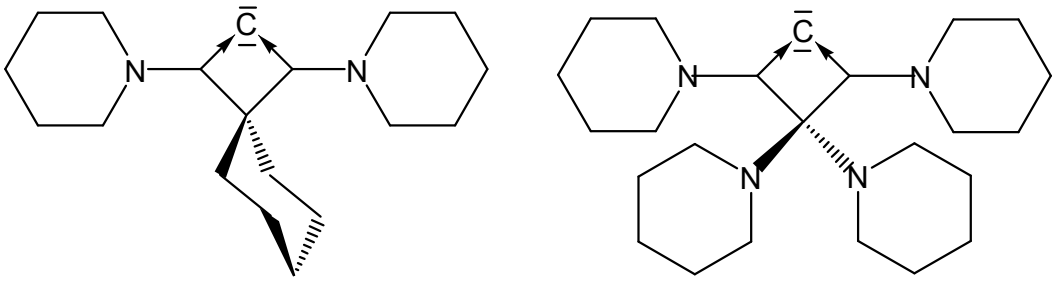

6a
Bertrand

6b
Tamm

Figure 8. Structures of compounds **6a** and **6b**.

The molecular orbitals show that the HOMO and HOMO-1 have clearly the largest coefficients at the central carbon atom and exhibit the typical shape of lone-pair molecular orbitals with σ (HOMO) and π (HOMO-1) symmetry; however, with reversed order with respect to CDPs and CDCs. To emphasize the proximity of **6** to CDP carbones, we use the same symbolism mimicking a metal.

The free CBA **6b** could not be obtained only the cationic $\mathbf{6bH^+}$ and $\mathbf{6bH_2^{2+}}$ are known and used as starting compounds for the syntheses of the related transition metal complexes [72].

Table 6. Transition metal complexes with the all carbon ligand **6**; ^{13}C NMR shifts (in ppm) of the donating carbon atom. Distances in Å, angles in°.

Nr.	^{13}C NMR	C-M	C-C	C-C-C	Ref.
	Transition metal complexes with the carbone **6a**				
6a-RhCl(cod)	136.6 (41)	2.038(5)	1.405(6)	88.4(3)	[71]
6a-IrCl(cod)	138.6	nr	nr	nr	[71]
6a-RhCl(CO)$_2$	124.7 (32)	nr	nr	nr	[71]
6a-IrCl(CO)$_2$	129.2	nr	nr	nr	[71]
	Transition metal complexes with the carbone **6b**				
6b-W(CO)$_5$	130.1	2.319(3)	1.419(4)	88.0(2)	[72]
6b-AuCl	123.6	2.001(4)	1.409(5)	90.5(3)	[72]
6b-RhCl(CO)$_2$	131.2 (32)	2.0602(14)	1.4102(19)	89.73(11)	[72]

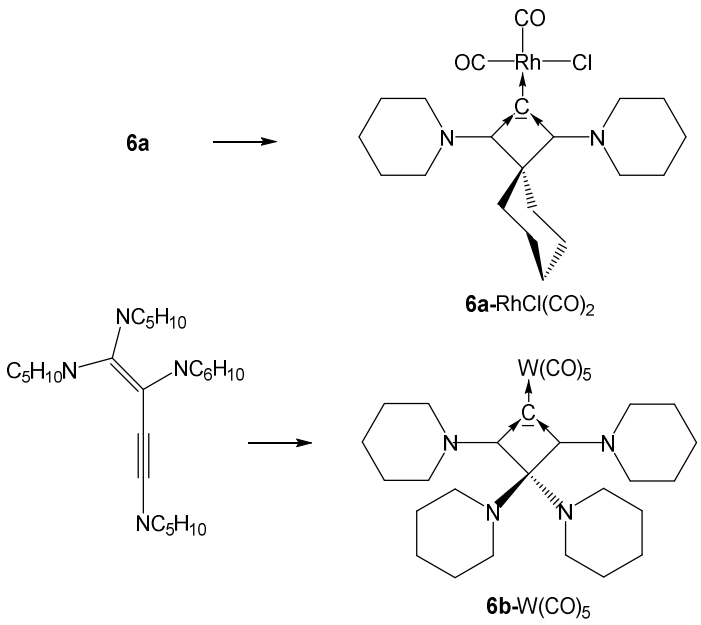

Scheme 14. Selected structures of complexes with the cyclic carbones **6a** and **6b**. Preparation see text.

The ^{13}C NMR shifts of the central carbon atom are shifted to higher fields relative to the starting free carbone ranging between 124 and 139 ppm.

All complexes of the CBA **6a** where obtained by reacting the freshly prepared free carbone **6a** at -20º with [{MCl(cod)}$_2$] with M = Rh, Ir. The cod ligand can be replaced by bubbling CO through solutions of **6a**-MCl(cod) to produce the related **6a**-MCl(CO)$_2$ compounds [71].

Transition metal complexes with **6b** as ligand where obtained by reacting 1,1,2,4-tetrapiperidino-1-buten-3-yne with a) [(tht)AuCl], b) [RhCl(CO)$_2$]$_2$, c) [(NMe$_3$)W(CO)$_5$]; during the reaction rearrangement of the starting buten-3-yne to **6b** has occurred [72].

2.7. Cyclopropenylidene

Stephan described the first carbodicarbene stabilized by flanking cyclopropylidenes, named carbodicyclopropylidene **7**.

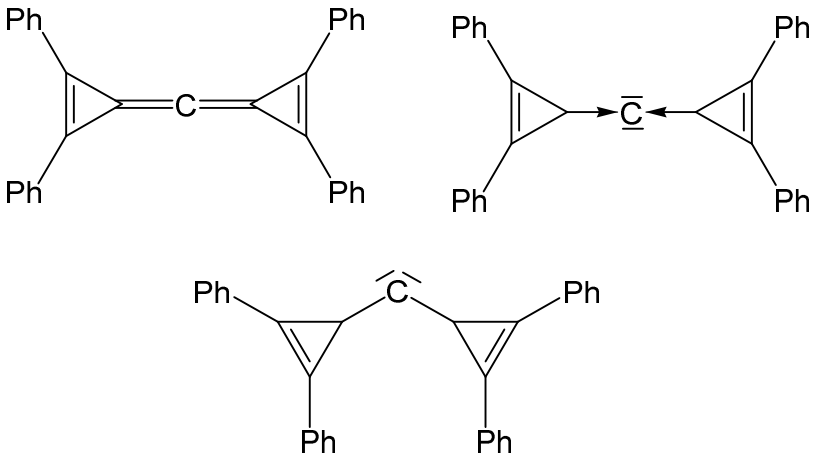

7

Stephan

Figure 9. Possible description of the bonding in **7**.

Neither the neutral singlet 1,2-diphenylcyclopropenylidene as carbene ligand L in 7 nor the carbone tetraphenylcarbodicyclopropenyliden (CDC) **7** itself are stable compounds at room temperature. The free carbene L has only been observed in an argon matrix isolated at 10 K and **7** could be characterized in solution by low temperature NMR spectroscopy; for the central carbon atom a ^{13}C NMR shift at δ = 133 ppm was recorded at −60°C.

The first and second proton affinities of **7** were determined to be 283 and 153 kcal mol^{-1}, respectively. Thus, the energy difference between the linear allenic structure and the bent arrangement is shallow amounting to 6.6 kcal mol^{-1} for a bending angle of 140 ° and 10 kcal mol^{-1} for 130°. The molecular structure of **7** was determined by computational methods. Calculations reveal that the central carbon atom is in a linear environment the C-C distances were calculated at 1.308 Å and the C-C-C angle to 180 º. The highest occupied molecular orbital (HOMO) and HOMO-1 of 2 are degenerate and incorporate the p orbitals of the C2-C1-C2a fragment.

The central C atom is more negatively charged (- 0.19 a.u.) than the adjacent C atoms suggesting nucleophilic character [73].

Table 7. Complexes with the carbone **7.** ^{13}C NMR shifts (in ppm) of the donating carbon atom.

Nr	^{13}C NMR	M-C	C-C	C-C-C	Ref.
[**7**-AuNHC-Ad]$^+$	92.7	2.071(6) 2.047(6)	nr	nr	[73]
[**7**-AuNHC-Dipp]$^+$	98.0	nr	nr	nr	[73]

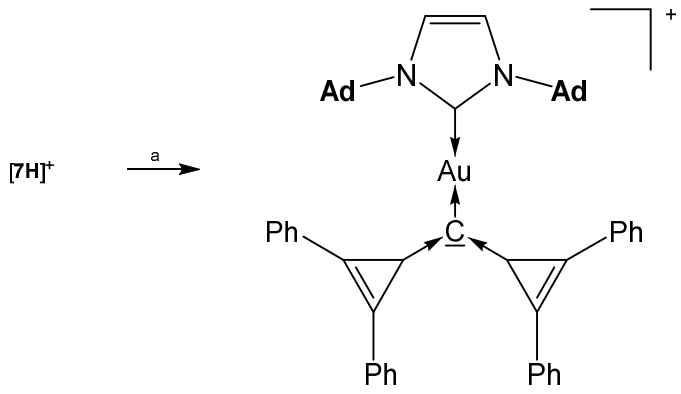

7-AuNHC-Ad

Scheme 15: Selected structures of complexes with the cyclo propylidene stabilized carbone 7. a) KHMDS/ (NHC)AuOTf.

The addition compounds [**7**-AuNHC-Ad]OTf and [**7**-AuNHC-Dipp]OTf were prepared from reacting [**7H**]$^+$ with KHMDS and the related (NHC)AuOTf at -45º [73].

2.8. Carbodicarbenes

Carbodicarbenes, CDCs, are neutral compounds, where a bare carbon atom with its four electrons is stabilized by two NHC ligands which plays the role of a phosphine group as in carbodiphosphoranes, CDPs. Theoretical studies have demonstrated that this class of compounds could be stable and their existence was predicted by Frenking [74] and short times later realized by the group of Bertrand [75].

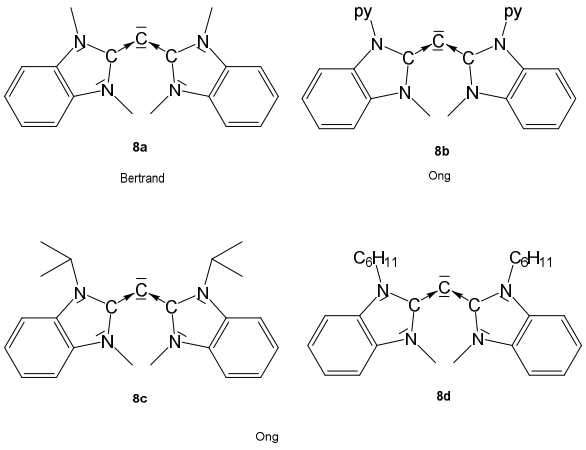

Figure 10. Symmetrical CDCs from which transition metal complexes are known.

Structural and spectroscopic parameters of the following symmetric CDCs are available: **8a,** C-C = 1.343(2) Å, C-C-C = 134.8(2)º, ^{13}C NMR 110.2 ppm [75]. **8b,** C-C = 1.333(2) Å and 1.324(2) Å, C-C-C = 143.61(15)º [76]**. 8c,** C-C = 1.335(5) Å, C-C-C = 136.6(5)º [77].

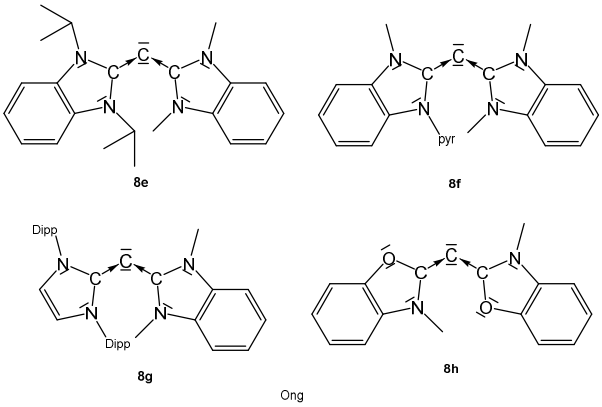

Figure 11. Unsymmetrical CDCs from which transition metal complexes are reported.

Structural parameters of the unsymmetrical CDCs are reported: **8e,** C-C = 1.3401(16) Å and 1.3455(16), C-C-C 137.55(12)º. For **8f**, no data are available [78].

8g: C-C = 1.344(3) Å and, 1.318(3) Å, C-C-C = 146.11(19)º [78]. **8h** was obtained at -60º by reacting **8hH**$^+$ with KMDS, and characterized spectroscopically; on warming to room temperature, it dimerizes. ^{13}C NMR: δ = 105.5 ppm [79].

Table 8. Collection of transition metal complexes with the CDCs **8a-8h**. ^{13}C NMR shifts of the central carbon atom (in ppm).

Nr	^{13}C NMR	M-C	C-C	C-C-C	Ref.
Transition metal complexes with the CDC **8a**					
8a-RhCl(CO)$_2$	64.1	2.089(7)	1.398(10)	121.2(7)	[75]
8a-RuCl$_2$(=CHPh)NHC	73.01 mes	2.2069(18)	1.352(3) 1.429(3)	119.84(17)	[80]
8a-RuCl$_2$(=CHPh)NHC	73.4 ^{i}Pr	2.210(7)	1.345(11) 1.439(9)	116.9(6)	[80]
Transition metal complexes with the CDC **8b**					
[**8b**-PdCl]$^+$	nr	1.973(3)	1.369(5) 1.398(5)	126.5(3)	[76]
[**8b**-Fe$_{0.5}$]$^{2+}$		2.018(3)	1.374(3)	128.4(3)	[81]
[**8b**-Fe$_{0.5}$]$^{3+}$		1.968(4)	1.387(6)	125.2(4)	[81]
[**8b**-Fe$_{0.5}$]$^{4+}$		1.928(3)	1.407(4)	125.4(2)	[81]
Transition metal complexes with the CDC **8c**					
8c-PdClC$_3$H$_5$	nr	2.207(4)	1.404(5) 1.377(5)	119.7(4)	[77]
8c-RhCl(CO)$_2$	63.7	2.109(2)	1.4113) 1.385(3)	117.4(2)	[77]
Transition metal complexes with the CDC **8d**					
8d--RhCl(CO)$_2$		2.123(2)	1.416(3) 1.368(3)	116.8(2)	[77]
Transition metal complexes with the asymmetric CDC **8e**					
8e-PdCl$_2$(POR)$_3$	nr	2.0398(18)	1.395(3) 1.328(3)	119.20(16)	[82]
8e-PdCl$_2$PPh$_3$	nr	2.063(2)	1.383(3) 1.409(3) tP	115.63(19)	[83]
8e-PdCl$_2$PTol$_3$	nr	2.049(4)	1.374(7) 1.412(8) tP	117.7(4)	[83]
8e-PdCl$_2$PCy$_3$	nr	2.111(2)	1.343(3) 1.415(4) tP	123.6(2)	[83]
Transition metal complexes with the asymmetric CDC **8f**					
8f-RhCl(CO)$_2$	67.1	2.117(2)	1.369(3) 1.424(3)	117.8(2)	[78]
Transition metal complexes with the asymmetric CDC **8g**					
8g-RhCl(CO)$_2$	63.2	2.1164(17)	1.374(2)$_{NHC}$ 1.420(3)	118.77(16)	[78]
Transition metal complexes with the asymmetric CDC **8h**					
8h-IrCl(CO)$_2$	nr	nr	nr	nr	[79]
8h-IrCl(cod)	166.4	nr	nr	nr	[79]

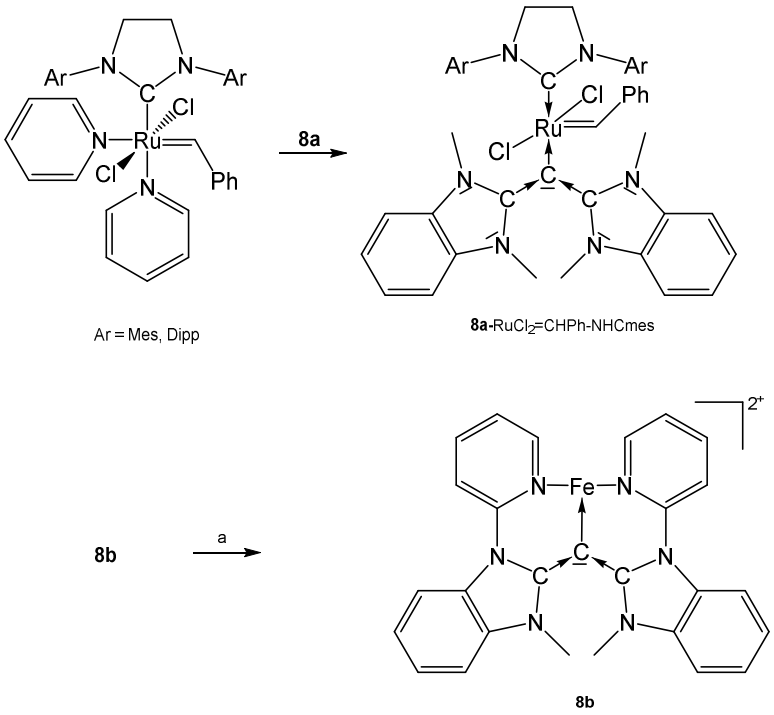

Scheme 16. Selected structures of transition metal complexes with symmetric CDCs **8a** and **8b**; a) $Fe(OTf)_2(MeCN)_2$

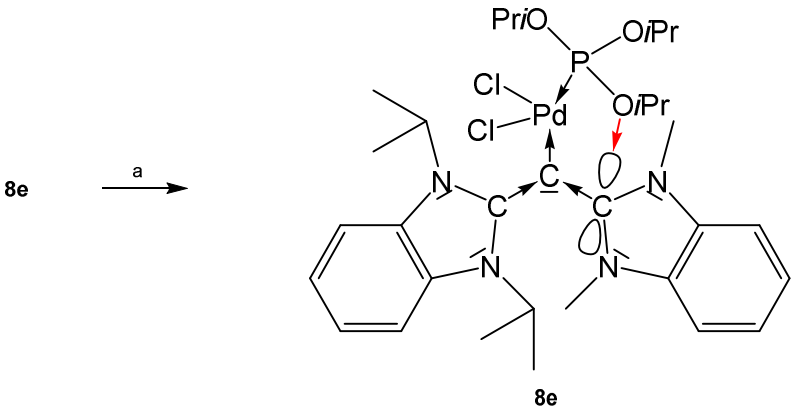

Scheme 17. Selected structural representation of **8e**-$PdCl_2P(OiPr)_3$ a) $PdCl_2P(OiPr)_3$

8a-$RhCl(CO)_2$ was prepared by addition of a suspension of **8a** in benzene to a solution of $[RhCl(CO)_2]_2$ [75]. **[8b**-$Fe_{0.5}]^{2+}$ contains Fe^{2+} in octahedral environment coordinated by two molecules of **8b**. Fe(II) can be successively oxidized to the corresponding tri-, tetra-, and pentacationic species [81].

The addition compounds **8c**-$RhCl(CO)_2$ and **8d**-$RhCl(CO)_2$ where obtained upon reacting the appropriate carbone **8c** or **8d** with $[RhCl(CO)_2]_2$; similarly addition of $[Pd(allyl)Cl]_2$ to **8c** leads to the allyl complex **8c**-$PdCl(C_3H_5)$ [77].

As depicted in **Scheme 17**, introduction of $PdCl_2P(OiPr)_3$ to **8e** afforded the complex **8e**-$PdCl_2P(OiPr)_3$; it features a square planar Pd center with a short interatomic distance of one phosphite oxygen atom and the carbon atom of the NHC molecule of 2.890 Å that is smaller than the sum of van der Waals radii. This indicates strong attractive interaction between the atoms [82]. The three Pd complexes **8e**-$PdCl_2PPh_3$, **8e**-$PdCl_2PTol_3$, and **8e**-$PdCl_2PCy_3$ were obtained by reacting the carbone **8e** with the appropriate $PdCl_2PR_3$; between the NHC and the aromatic phosphine substituents (Ph or Tol) an unexpected π-π interaction was detected. One Ph and Tol group are nearly parallel to the imidazole rings with centroid-centroid distances of 3.25 Å (Ph) and 3.30 Å (Tol), respectively [83].

8f –$RhCl(CO)_2$ and **8g**-$RhCl(CO)_2$ stem from reacting the appropriate carbone with $[RhCl(CO)_2]_2$ [78]. The cod ligand of $[Ir(cod)Cl]_2$ was replaced by bubbling CO through a mixture with **8h** to generate the complex **8h**-$IrCl(CO)_2$ [79].

2.9. Tridentate cyclic diphosphino CDCs

The carbones **9a** and **9b** are functionalized carbodicarbene in which the donating carbon atom is part of a seven membered ring.

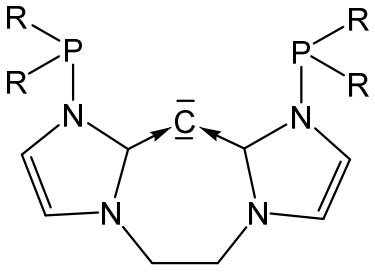

9a, R = Ph
9b, R = Pr^i

Meek

Figure 12. Hypothetical free carbones **9a** and **9b**.

The neutral **9a** and **9b** could not be isolated, source for transition metal complexes are the related cations **9aH**$^+$ and **9bH**$^+$ [84].

Table 9. Transition metal complexes with the carbones **9a** and **9b**; ^{13}C NMR signal of the central donating carbon atom.

Nr	^{13}C NMR	M-C	C-C	C-C-C	Ref.
Transition metal complexes with the carbone **9a**					
9a-RhCl	73.0	nr	nr	nr	[84]
[**9a**-RhNCMe]$^+$	nr	2.043	1.398 1.387		[84]
[**9a**-Rh(CO)]BF_4	nr	nr	nr	nr	[84]
[**9a**-Rh(styrene)]BF_4	nr	2.075(2)	1.404(3) 1.391(3)	121.7(2)	[85]
[**9aH**-Rh(CO)]$(BF_4)_2$	nr	nr	nr	nr	[85]
Transition metal complexes with the carbone **9b**					
9b-RhCl	73.4	nr	nr	nr	[84]
[**9b**-RhNCMe]BF_4	nr	nr	nr	nr	[84]
[**9b**-Rh(CO)]BF_4					[84]

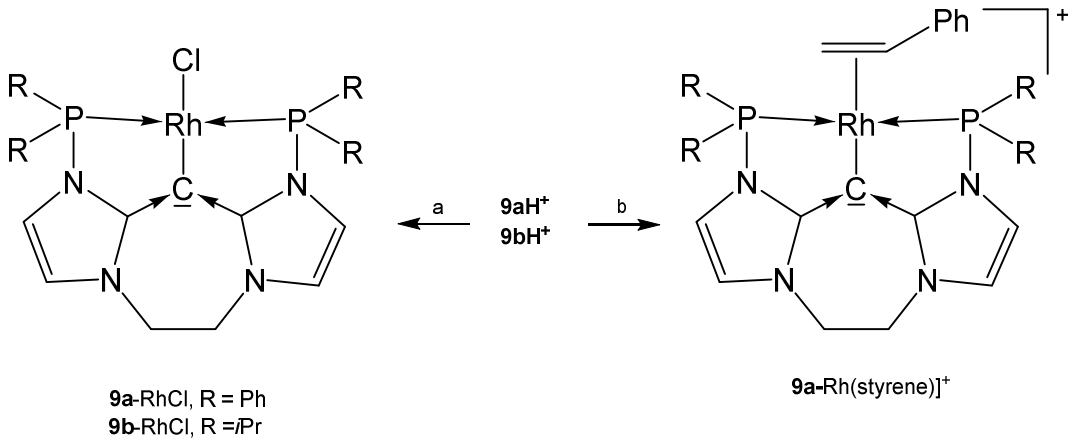

9a-RhCl, R = Ph
9b-RhCl, R = *i*Pr

9a-Rh(styrene)]$^+$

Scheme 18. Selected structures of transition metal complexes with the carbones **9a** and **9b**. a) $[Rh(cod)Cl]_2$/NaOMe, b) **9a**-RhCl/styrene/$NaBF_4$.

The neutral complexes **9a**-RhCl and **9b**-RhCl where prepared upon reacting the cations **9aH**$^+$ or **9bH**$^+$, respectively with $[Rh(cod)Cl]_2$/NaOMe; if treated with $AgBF_4$/MeCN the cationic spezies [**9a**-Rh(MeCN)]BF_4 and [**9b**-Rh(MeCN)]BF_4, respectively, were isolated. The related carbonyl complexes [**9a**-Rh(CO)]BF_4 and [**9b**-Rh(CO)]BF formed similarly upon reaction with $[Rh(CO)_2Cl]_2$/NaOMe [84]. The styrene complex [**9a**-Rh(styrene)]$^+$ was obtained upon treating the related chloro complex with styrene/$NaBAr_4$; the styrene complex catalyzes

the hydroarylation of dienes. Protonation of [**9a**-Rh(CO)]+ with HBF_4 OEt_2 generates **[9aH**-Rh(CO)]$^{2+}$ in which the carbone acts as four electron donor [85].

2.10. Tetraaminoallene (TAA) transition metal complexes

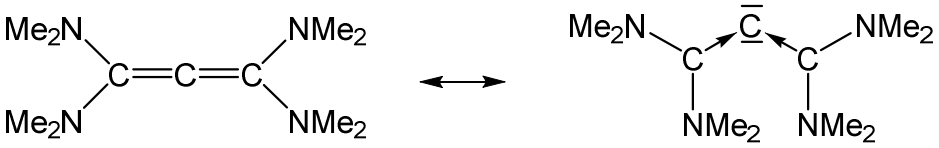

10

Figure 13. Linear tetraaminoallene (TAA) and the extreme formulation as a carbodicarbene with a bent array. TAA's has hidden or masked pairs of electrons.

The ^{13}C NMR shift of the central carbon atom amounts to 142.8 ppm. The first and second PAs of **10** are 282.5 and 151.6 kcal/mol, respectively [16,74].

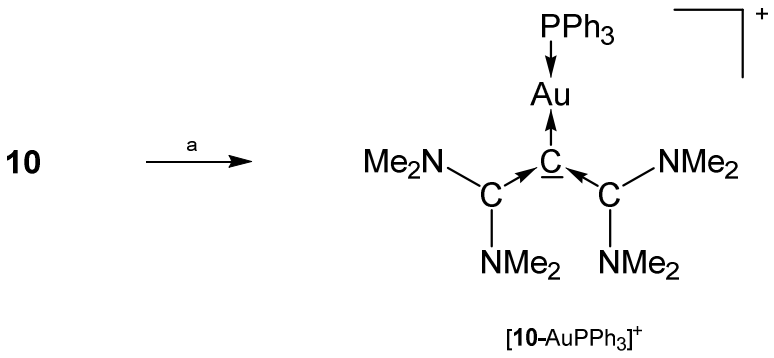

[**10**-AuPPh$_3$]$^+$

Scheme 19: Structure of [**10**-AuPPh$_3$]SbF$_6$; a) AuClPPh$_3$/NaSbF$_6$

The salt [**10**-AuPPh$_3$]SbF$_6$ is the only transition metal complex of TAA, which has been reported so so far. Both carbene moieties are planar, but are tilted relative each other, to relieve allylic strain [86]. The Au-C bond lengths amounts to 2.072(3) Å and the slightly different C-C dative bonds has interatomic distances of 1.406(5) and 1.424(5) Å. The central C-C-C bond angle is reported with 118.5(3)°.

2.11. Transition metal complexes of carbones with the P-C-C skeleton

Mixed carbene-phosphine stabilized carbones from the working group of Bestmann (1974) and Alkarazo (2009).

11a Bestmann

11b Alkarazo

Figure 14. In compounds **11** the C(0) is stabilized by a phophine and a carbene ligand.

The crystal structure of **11a** reveals a planar configuration of the carbene ligand $C(OEt)_2$. Short P-C and C-C distances indicate some p back donation; P-C = 1.682(4)Å, C-C = 1.316(10) Å, C-C-C 125.6º [87].

Table 11. Transition metal complexes with the mixed carbones **11a** and **11b.** ^{31}P NMR shifts in ppm.

Nr	^{31}P NMR	M-C	P-C C-C	P-C-C	Ref.
Transition metal complexes with the carbone **11a**					
11a-$RhCl(CO)_2$	25.1	nr	nr-	nr	[88]
11a-AuCl	26.7	2.014916)	1.7449(16) 1.362(2)	114.30(12)	[88]
11a-$(AuCl)_2$	28.1	2.081(4) 2.103(4)	1.785(4) 1,425(6)	114.2(3)	[88]
Transition metal complexes with the carbone **11b**					
11b-AuCl	22.2	nr	nr	nr	[88]

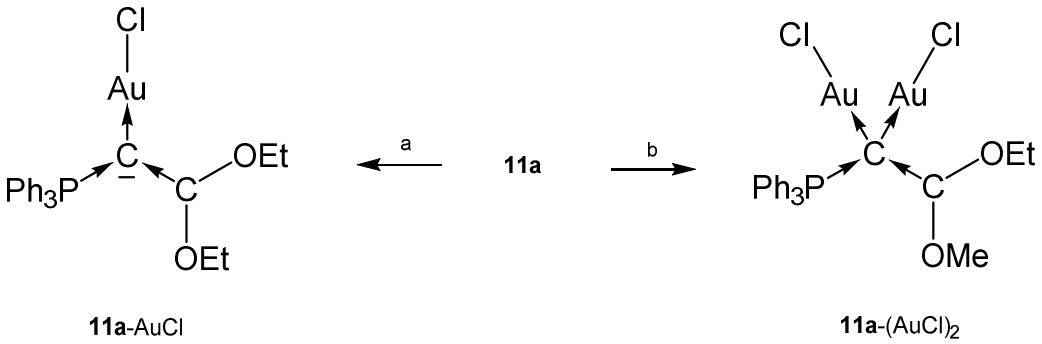

11a-AuCl **11a**-$(AuCl)_2$

Scheme 20. Selected structural representation of transition metal complexes of **11a**. a) one equiv. of $AuCl(SMe_2)$, b) two equiv. of $AuCl(SMe_2)$.

The neutral Rh complex **11a**-$RhCl(CO)_2$ was obtained from reacting the carbone **11a** with $[Rh(CO)_2Cl]_2$. Similarly, the complex **11b**-AuCl results from reaction of **11b** with $AuCl(SMe_2)$ [88].

2.12. Transition metal complexes of carbones with the P-C-Si skeleton

The neutral compound **12** is a carbone in which the C(0) atom is stabilized by a donor stabilized silylene and a phosphine ligand.

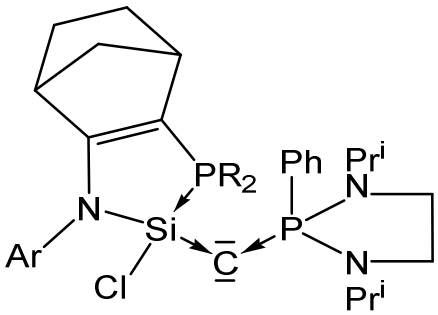

12

Kato

Figure 15. Carbone complex reported by Kato et al [89].

The crystal structure of a related compound to **12** (a cyclopentene instead of a cyclohexene ring) shows a P-C distance of 1.6226(4) Å and Si-C distance of 1.6844(4) Å; the Si-C-P angle amounts to 140.03(3)º. Addition of CuCl generates the complex **12**-CuCl. No spectroscopic or structural details are available [89].

2.13. Transition metal complexes of carbones with the P-C-S skeleton

A series of carbones (**13a** to **13c**) based on a P-C-S core containing the neutral S(IV) ligands SPh_2=NMe (Figure 16) were reported by Fujii [90].

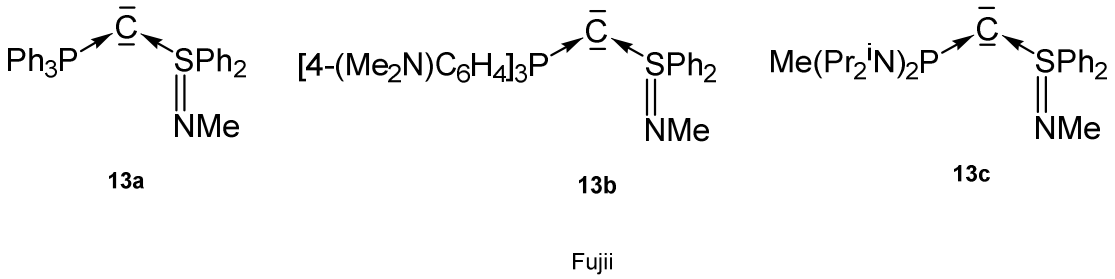

Figure 16. Carbone complexes reported by Fujii et al [90].

Crystal structures and ^{31}P NMR shifts of the following basic carbones are available: **13a,** δ = -2.64 ppm; **13b** δ = -1.39 ppm, P-C = 1.663(2) Å, S-C 1.602(2) Å, P-C-S = 125.59(15)º. The authors revealed a high electron density at the central carbon atom.

Table 12. Collection of transition metal complexes with the carbones **13a** to **13c**. ^{31}P NMR signals (in ppm) are given.

Nr	^{31}P NMR	M-C	P-C	S-C	P-C-S	Ref
Transition metal complexes with the carbone **13a** based on a P-C-S core						
13a-AgCl	10.8	2.131	1.711	1.648	121.9	[90]
[**13a**-$AuPPh_3$]OTf	15.2	nr	nr		nr	[90]
[**13a**-$(AuPPh_3)_2$]OTf_2	29.7	nr	nr		nr	[90]
Transition metal complexes with the carbone **13b** based on a P-C-S core						
13b-AgCl	9.13	2.098	1.728	1.636	119.1	[90]
[**13b**-$AuPh_3$]OTf	12.88	nr	nr		nr	[90]
[**13b**-$(AuPPh_3)_2$]OTf_2	27.45	2.127 2.118	1.788	1.737	115.6	[90]
13b-Ag-**13b**	8.43	2.160	1.707	1.635	121.8 127.0	[90]
13b-$HAuPPh_3$	17.1	2.106	1.817	1.782	116.3	[90]
Transition metal complexes with the carbone **13c** based on a P-C-S core						
13c-$CuN(SiMe_3)_2$						[90]

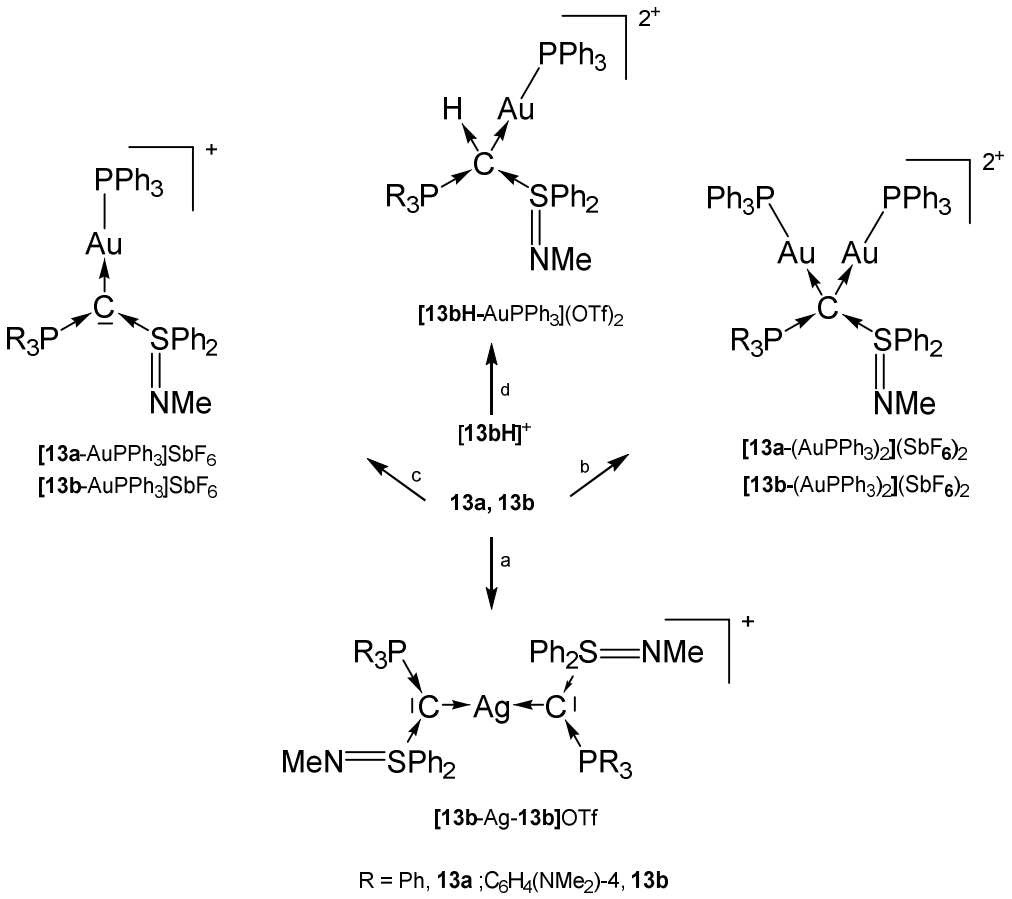

Scheme 21. Selected structures with the carbones **13a** und **13b**: a) 0.5 eq. of AgOTf, b) 2 eq. of $AuCl(PPh_3)$/ 2 eq. of $AgSbF_6$, c) 1 eq. of $AuCl(PPh_3)$/ 1 eq. of $AgSbF_6$, d) ion exchange (OH^- form), 1 eq. of $AuClPPh_3$/ 1 eq. of AgOTf [90].

The addition products **13a-**AgCl and **13b-**AgCl were obtained from reacting [**13aH**]$^+$ or [**13bH**]$^+$, respectively with ion exchange resin (Cl^- form) and Ag_2O/CH_2Cl_2. For the other products, see Scheme 21 [90].

Addition of TM fragments to **13a** or **13b** elongates P-C and S-C bond length as reported for **1a.** That of **[13bH-**$AuPPh_3$**]**$(OTf)_2$ in which **13b** acts as four electron donor are elongated to normal single bonds [90].

2.14. Transition metal complex with a P-C-S core possessing a neutral S(II) ligand

The carbone **14** contains a phosphine and a S(II) ligand with a free pair of electrons to stabilize the C(0) atom. However, the bare **14** could not be isolated, but only the protonated cation [**14H**]$^{+}$ and used as starting material [91].

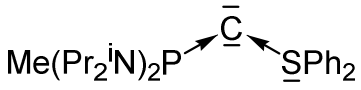

14

Baceiredo

Figure 17. Mixed P and S stabilized carbone **14**.

The transition metal complex [**14**-CuN(SiMe$_3$)$_2$]OTf was prepared upon reacting [**14H**]+ with KHMDS/CuCl. X-ray analysis reveals a Cu-C distance of 1.903(4) Å and the P-C and S-C distances amount to 1.709(5) and 1.677(5) Å, respectively. As found in carbone addition compounds of **13a** and **13b** the P-C distance is longer than the S-C distance. An acute P-C-S angle of 115.3(2)º was recorded. The ^{31}P NMR signal is shifted to lower fields at 66.5 ppm [91].

2.15. Transition metal complexes of carbones with the S-C-S skeleton

In the carbones **15** (carbodisulfanes, CDS) the central carbon atom is stabilized by two neutral S(II) ligands (**15a**), or S(II), S(IV) groups (**15b**) or two S(IV) (**15c**) ligands.

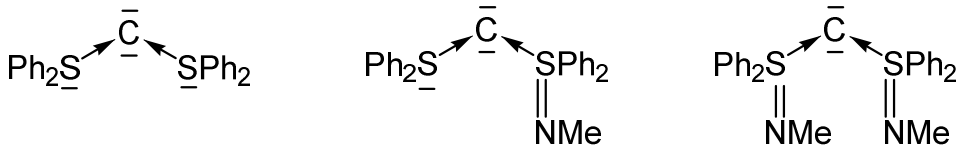

15a **15b** **15c**

Fujii

Figure 18. Sulfur based carbones **15** as ligands for transition metal complexes.

The molecular structure of **15a** was investigated computationally [92]. For the carbones the following parameters were recorded: **15b,** C-S^{II} 1.707(2), C-S^{IV} 1.648(2), S-C-S 106.67(14). ^{13}C NMR, d = 35.4 ppm [93]. **15c**: S-C 1.635(4), 1.636(2); S-C-S 116.8(2) [94].

Similar to CDCs the first and second PAs of **15b** amount to 288.0 and 184.4 kcal/mol, respectively.

Table 13. Transition metal complexes with selected bond length (Å) and angles (deg) of the carbone ligands **15a** to **15c**. ^{13}C NMR signal (in ppm) of the central carbon atom.

Transition metal complexes with the CDS **15a**					
	^{13}C NMR	**C-M**	**S^{II}-C**	**S^{II}-M-S^{II}**	**Ref.**
15a-AgCl	not obs	2.058(8)	1.707(8) 1.698(8)	107.3(5)	[92]
[15a-AuPPh$_3$]OTf	65.4	-	-	-	[92]
[15a-(AuPPh$_3$)$_2$]$^{2+}$	not obs	2.116(6) 2.084(5)	1.782(6) 1.767(6)	115.4(3)	[92]
[15aH-AuPPh$_3$]$^{2+}$	66.0	2.090(7)	1.837(7) 1.805(7)	104.4	[92]
Transition metal complexes with the CDS **15b**					
	^{13}C NMR	**C-M**	**S^{II}-C** **S^{IV}-C**	**S^{II}-M-S^{IV}**	
[15b-AuPPh$_3$]OTf	67.4	-	-	-	[92]
[15b-Ag-**15b**]OTf	not obs	2.111(7) 2.097(7)	1.718(6) 1.664(7)	106.3(6)	[92,95]
[15b-(AuPPh$_3$)$_2$]$(OTf)_2$	not obs	2.130(3) 2.103(3)	1.792(3) 1.746(3)	106.27(18)	[92]
[15b-Ag$_2$-**15b]**$(OTf)_2$	not obs	-	-	-	[95]
[15b-Ag$_4$-**15b**]$(OTf)_4$	not obs	2.192 2.187			[95]
[15bH-AuPPh$_3$]$(OTf)_2$	72.1	2.098(3)	1.796(3) 1.789(3)	106.83(17)	[92]
Transition metal complexes with the CDS **15c**					
		C-M	**S^{IV}-C**	**S^{IV}-M-S^{IV}**	
[15c-AuPPh$_3$]OTf	65.1	-	-	-	[92]
15c-AgCl	not obs	2.134(3)	1.690(3) 1.678(3)	112.16(14)	[92]
[15c-(AuPPh$_3$)$_2$]$(OTf)_2$	not obs	2.126(4) 2.125(4)	1.789(4) 1.735(5)	112.5(2)	[92]
[15c-Ag-**15c**]OTf	40.0	2.116 2.127	1.671-1.696	114.6 115.6	[95]
[15c-Ag$_2$-**15c]**$(OTf)_2$	43.1	2.147	1.666 1.696	114.7	[95]
[15c-Ag$_4$-**15c**]$(OTf)_4$	nr	2.228 2.193	nr	nr	[95]
{[**15c**(AuPPh$_3$)$_2$AgOTf](OTf)$_4$}$_2$	nr	2.139 2.108	1.757 1.747	116.8	[92]

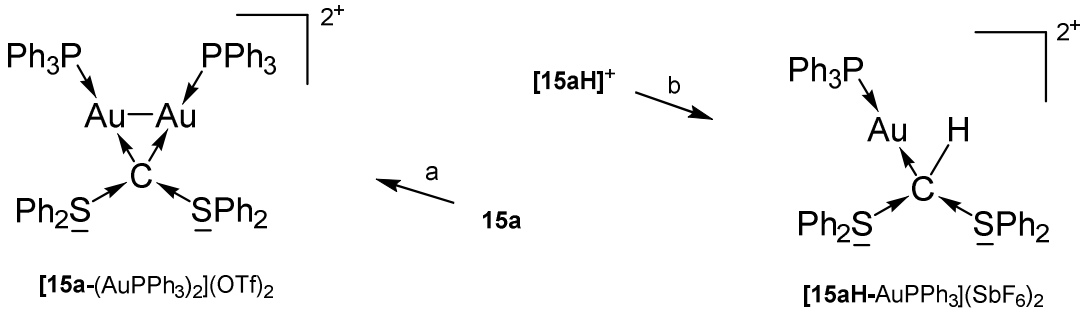

Scheme 22. Selected of complexes with the carbone **15a.** a) 2 eq AuCl(PPh$_3$), b) AuCl(PPh$_3$)$_2$.

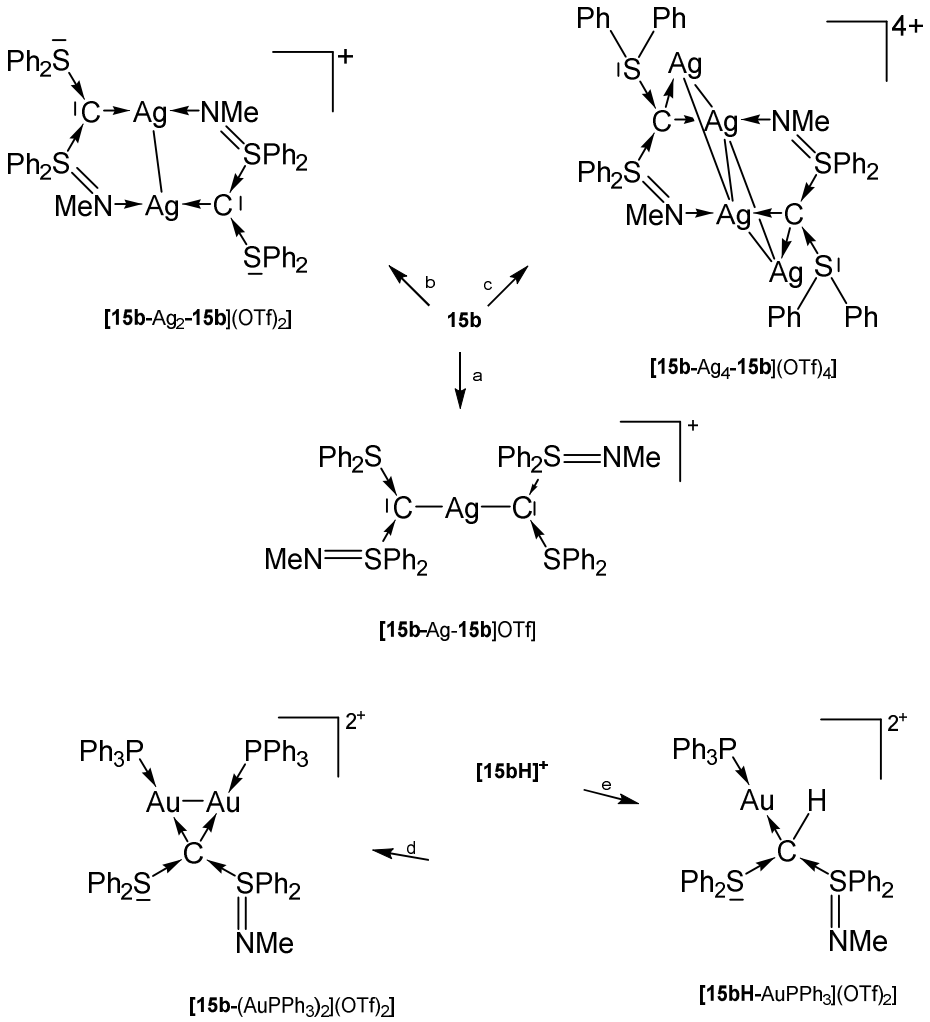

Scheme 23. Selected of complexes with the carbone **15b.** a) 0.5 eq AgOTf, b) 1.0 eq AgOTf, c) 2.0 eq AgOTf, d) 2 eq AuCl(PPh$_3$), e) AuCl(PPh$_3$).

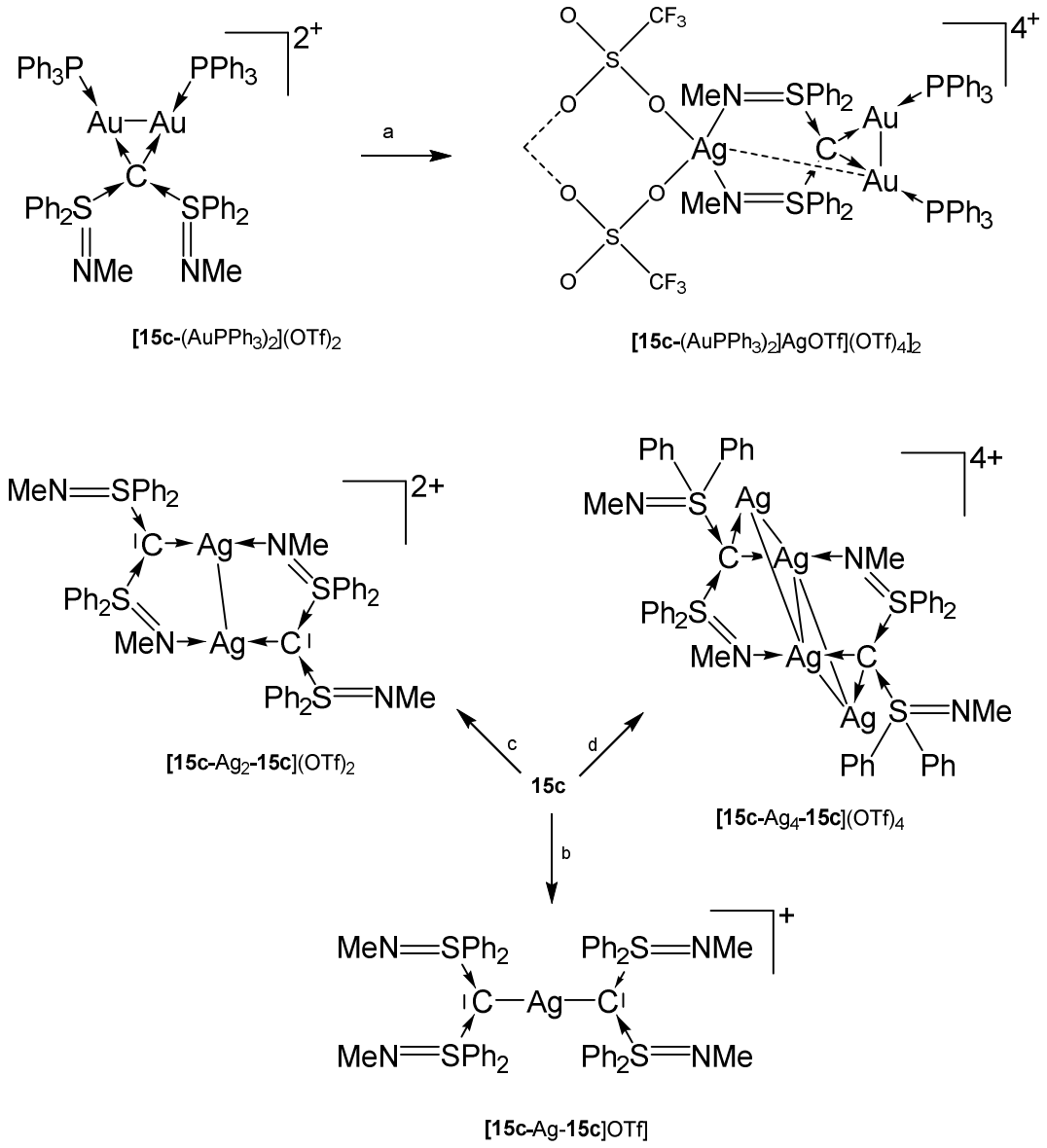

Scheme 24. Selected complexes with the carbone ligand **15c**; a) AgOTf, b) 0.5 eq AgOTf, c) 1.0 eq AgOTf, d) 2.0 eq AgOTf. {[**15c**-$(AuPPh_3)_2$AgOTf]$(OTf)_4$}$_2$ is dimeric linked by two OTf anions.

15a-AgCl was obtained from [**15aH**]$^+$ upon treating with Ag_2O/CH_2Cl_2. The salt [**15a**-$AuPPh_3$]OTf formed reacting the bare **15a** with $AuCl(PPh_3)$ followed by addition of NaTfO in THF. [**15a**-$(AuPPh_3)_2$]$(OTf)_2$ and [**15aH**-$AuPPh_3$](SbF_6) are sketched in Scheme 22 [92].

[**15b**-$AuPPh_3$]OTf was obtained analogously formed from reacting **15b** with $AuCl(PPh_3)$ followed by addition of NaTfO in THF. For the other compounds, see Scheme 23 [92].

The preparation of **[15c-**$AuPPh_3$]OTf and **15c-**AgCl follows the procedure outlined for the related **15b** compounds [92]. For the other compounds, see Scheme 24 [92,95]. The hetero hexametallic cluster {[**15c-**$(AuPPh_3)_2$AgOTf](OTf)$_4$}$_2$ is supported by two carbone ligands that adopt a κ^4*C,C',N,N'* coordination mode. The Au---Ag separation amounts to 3.003 Å [92].

^{13}C NMR signals of the donating C(0) atoms (if available) of all addition compounds of **15a** to **15c** are less shielded than that of the basic carbones [92].

2.16. Transition metal complexes of carbones with the S-C-Se skeleton (16)

Compound **16** is the first carbone containing a Se(II) compound together with a S(IV) one as ligand for stabilization of a C(0) atom.

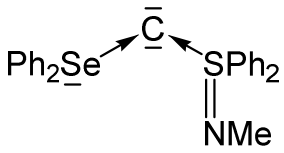

16

Fujii

Figure 19. Carbone with Se and S based ligands L.

Table 14. Transition metal complexes with selected bond length (Å) and angles (deg) of the carbone **16** ^{13}C NMR signal (in ppm) of the central carbon atom.

	^{13}C NMR	**C-M**	**C-S** **C-Se**	**S-C-Se**	**Ref.**
[**16-**Ag-**16**]OTf	not obs.	nr	nr	nr	[95]
[**16-**Ag_2-**16**](OTf)$_2$	52.7	nr	nr	nr	[95]
[**16-**Ag_4-**16**](OTf)$_4$	not obs	2.174(5)	1.714(5) 1.923(6)	106.4(3)	[95]
[**16**H-Ag-**16**H]$(BF_4)_3$	not obs	2.164(4) 2.177(4)	1.772(5) 1.771(5) 1.936(4) 1.948(5)	103.8(2)	[93]

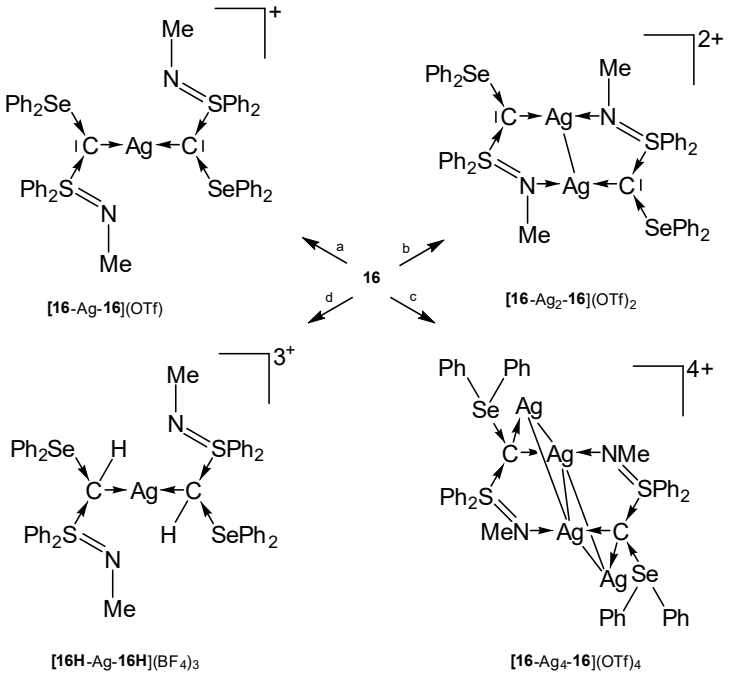

Scheme 25. Transition metal complexes with the carbone **16** as two and four electron donor. a) 0.5 eq AgOTf, b) 1 eq AgOTf, c) 2.0 eq AgOTf, d) $AgBF_4/CH_2Cl_2$.

The tetranuclear complex [**16**-Ag_4-**16**]$^{4+}$ contains a rhomboidal $[Ag_4]^{4+}$ core surrounded by two carbones **16**. In this and in [**16H**-Ag-**16H**]$^{3+}$ the donating C(0) acts as a four electron donor [95].

3. Transition metal carbido complexes [M]-C

The second part of this review summarizes the research of transition metal complexes with a naked carbon atom as ligand [M]-C. They are often termed as carbides but the bonding situation is clearly different from well-known carbides of the alkaline and alkaline earth elements E, which are salt compounds of acetylene E_nC_2. The electron configuration of carbon atom in the ^{1}D state ($2s^2 2p_x^2 2p_y^0 2p_z^0$) is perfectly suited for dative bonding with a transition metal following the DCD model [7] in terms of σ donation and π backdonation [M]⇄C|. Carbon complexes [M]-C may thus be considered as carbone complexes [M]-CL_2 without the ligands L at the carbon atoms. A theoretical study showed in 2000 that the 18 valence electron (VE) complex $[(CO)_4Fe(C)]$ is an energy minimum structure with a rather strong Fe-C bond [96]. However, such 18 VE systems could not be synthesized as isolated species but were only found as ligands where the lone-pair electron at the carbon atom serves as donor (see below). It

seems that the electron lone-pair at carbon in the 18 VE complexes [M]-C makes the adducts too reactive to become isolated.

It came as a surprise when Heppert and co-workers reported in 2002 the first neutral adducts with a naked carbon atom as a ligand, which are the formally 16 VE diamagnetic ruthenium complexes $[(PCy_3)LCl_2Ru(C)]$ (L= PCy and 1,3-dimesityl-4,5-dihydroimidazol-2-ylidene; Cy = Cyclohexyl) [22]. A subsequent bonding analysis of the model compound $[(Me_3P)_2Cl_2Ru\text{-}C]$ considered five different models A – E for the Ru-C bonds that are shown in Figure 20 [23]. It turned out that the best description for the bonding interactions is a combination of electron-sharing and dative bonds. An energy decomposition analysis [97] suggested that the model B provides the most faithful account of the bond, where the σ bond and the π bond in the Cl_2M plane come from electron-sharing interactions $Cl_2M{=}C$ whereas the π bond in the P_2M plane is due to backdonation $(Me_3P)_2Ru{\rightarrow}C$. The compounds $[(PCy_3)LCl_2Ru(C)]$ should therefore be considered as 18 VE Ru(IV) adducts. The following section summarizes the research of transition metal complexes with a naked carbon atom as ligand [M]-C that has been accomplished since 2002.

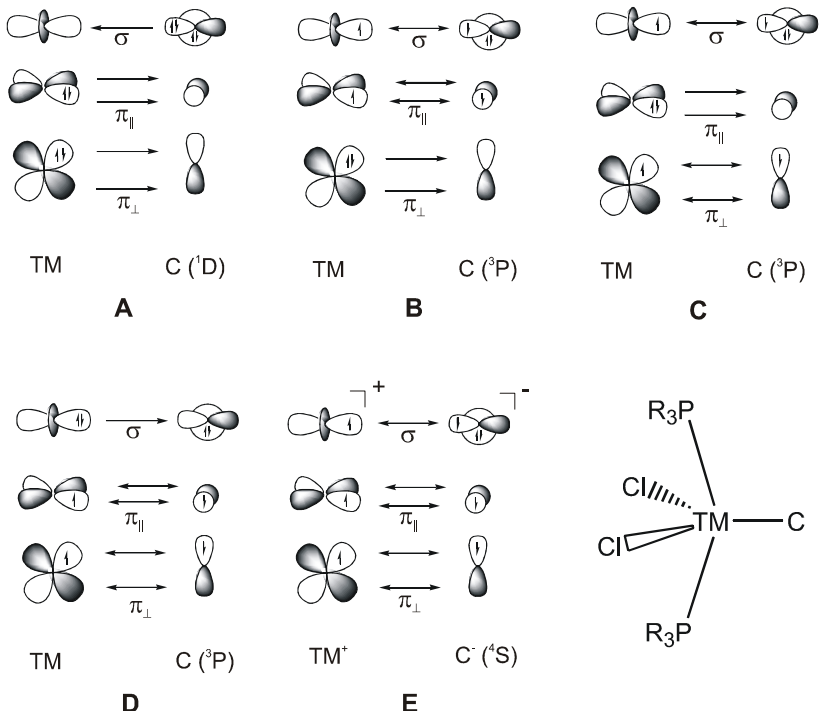

Figure 20. Bonding models A – E for the bonding between a transition metal (TM) and a naked carbon atom in the compound $[(R_3P)_2Cl_2Ru\text{-}C]$.

3.1. The system $RuCl_2(PCy_3)_2C$ ([Ru]C)

By far the most known complexes with carbido ligands that have been synthesized and structurally characterized are ruthenium adducts. The progress in the chemistry of ruthenium carbido complexes was reviewed in 2012 by Takemoto and Matsuzaka [121]. In the following we summarize the present knowledge on ruthenium carbido complexes, which was reported in the literature.

The X-ray analysis of [Ru]C exhibits a Ru-C distance of 1.632(6) Å. A signal at 471.8 ppm was attributed to the ligand carbon atom [98]. A general route to carbon complexes is described in [99].

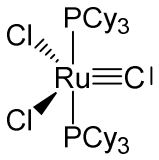

[Ru]C

Figure 21. The [Ru]C core

Addition of $PdCl_2(SMe_2)_2$ gives the complex [Ru]C→$PdCl_2(SMe_2)$, while with $Mo(CO)_5(NMe_3)$ the carbonyl complex [Ru]C→$Mo(CO)_5$ is generated [24,98]. A series of [Ru]C→$PtCl_2L$ complexes were obtained by Bendix from reacting the dimeric complex {[Ru]C→$PtCl_2]_2$ with various lígands L (L = PPh_3, PCy_3, $P(OPh)_3$, $AsPh_3$, CN^tBu, CNCy). Complexes with bridging Ligands L such as {[Ru]C→$PtCl_2]_2$bipy, {[Ru]C→$PtCl_2]_2$pyz, and {[Ru]C→$PtCl_2]_2$pym formed upon displacing ethylene from the related $(C_2H_4)PtCl_2$-L-$PtCl_2(C_2H_4)$ by [Ru]C. {[Ru]C→PtCl]$_2$(μ-Cl)pz results from an ethylene complex and [Ru]C as depicted in Scheme 26 [100]. A series of Pt, Pd, Rh, Ir, Ag, Ru complexes were presented by Bendix with X-ray data and ^{13}C NMR shifts of the ligand carbon atom ranging between 340 and 412 ppm [101]. Sulfur containing TM complexes with the metals Pd, Pt, Au, and Cu stem from the same laboratory. The sulfur ligands are ttcn = 1,4,7-trithiacyclononane and $S_4(MCp^*)_3$ (see Fig. 22) [102].

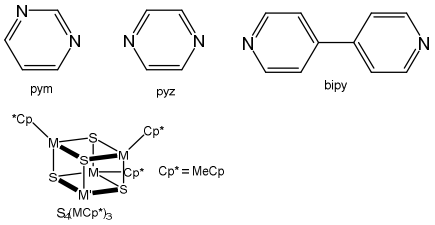

Figure 22. Spezification of ligands of Table 15.

Table 15. Selected structural (in Å and deg) and spectroscopic (^{13}C NMR in ppm) details of [Ru]C addition compounds

	^{13}C NMR	**Ru-C**	**M-C**	**Ru-C-M**	ref
[Ru]C→$PdCl_2(SMe_2)$	381.23	1.662(2)	1.946(2)	175.1(1)	[98]
{[Ru]C→$PdCl_3$}$^-$	380.9	nr	nr	nr	[101]
[Ru]C→$Mo(CO)_5$	446.31	nr	nr	nr	[98]
[Ru]C→$PtCl_2$Py	350.34	nr	nr	nr	[24]
					[100]
[Ru]C→$PtCl_2NCr(dbm)_2$	nr	1.676(2)	1.899(2)	174.5(1)	[24]
{[Ru]C→$PtCl_3$}$^-$	344.7	nr	nr	nr	[24]
					[101]
{[Ru]C→$PtCl_2$}$_2$	326.23	1.676(8)	1.871(8)	1796(4)	[24]
					[100]
[Ru]C→$PtCl_2PPh_3$	388.81	1672(2)	1.983(2)	173.7(1)	[100]
[Ru]C→$PtCl_2P(OPh)_3$	387.54	1.659(2)	2.001(2)	179.3(2)	[100]
[Ru]C→$PtCl_2AsPh_3$	374.68	1.670(2)	1.949(2)	171.9(2)	[100]
[Ru]C→$PtCl_2CN^tBu$	376.26	1.661(2)	1.967(6)	176.5(3)	[100]
[Ru]C→$PtCl_2CNCy$	376.04	nr	nr	nr	[100]
[Ru]C→$PtCl_2PCy_3$	396.77	1.666(3)	1.971(2)	174.5(2)	[100]
[Ru]C→$PtCl_2$(dmso)	349.0				[101]
{[Ru]C→$PtCl_2$}$_2$bipy	348.27	1.679(3)	1.891(4)	171.4(2)	[100]
{[Ru]C→$PtCl_2$}$_2$pyz	342.48	1.668(6)	1.895(6)	176.3(3)	[100]
{[Ru]C→$PtCl_2$}$_2$pym	341.36	1.678(3)	1.893(3)	176.0(2)	[100]
{[Ru]C→PtCl}$_2$(μ-Cl)pz	355.09	1.678(4)	1.909(4)	169.9(2)	[100]
[Ru]C→AuCl	395.3	nr	nr	nr	[101]
{[Ru]C→Au←C[Ru]}$^+$	395.3	nr	nr	nr	[101]
{[Ru]C→IrCl(CO)←C[Ru]}	397.4	nr	nr	nr	[101]
{[Ru]C→Rh(CO)}$_2$(μ-Cl)$_2$	396.4	nr	nr	nr	[101]
[Ru]C→RhCl(cod)	411.7	nr	nr	nr	[101]
[Ru]C→IrCl(cod)	387.6	nr	nr	nr	[101]
{[Ru]C→Ag(4'-H-terpy)}	433.5	nr	nr	nr	[101]
{[Ru]C→Ag(4'-Ph-terpy)}	433.1	nr	nr	nr	[101]
[Ru]C→Ag(ttcn)	nr	1.653(4)	1.876(4)	177.3(2)	[101]
[Ru]C→Cu(ttcn)	nr	1.622(7)	2.098(7)	176.9(5)	[101]
[Ru]C→Pd-S_4(MoCp*)$_3$	nr	1.672(3)	1.971(3	178.3(2)	[101]
[Ru]C→ Pt-S_4(MoCp*)$_3$	nr	1.689(7)	1.896(7)	178.2(5)	[101]
[Ru]C→ Pd-S_4(WCp*)$_3$	nr	1.668(5)	1.959(5)	178.1(3)	[101]
[Ru]C→ Pt-S_4(WCp*)$_3$	nr	1.699(9)	1.874(9)	178.8(6)	[101]

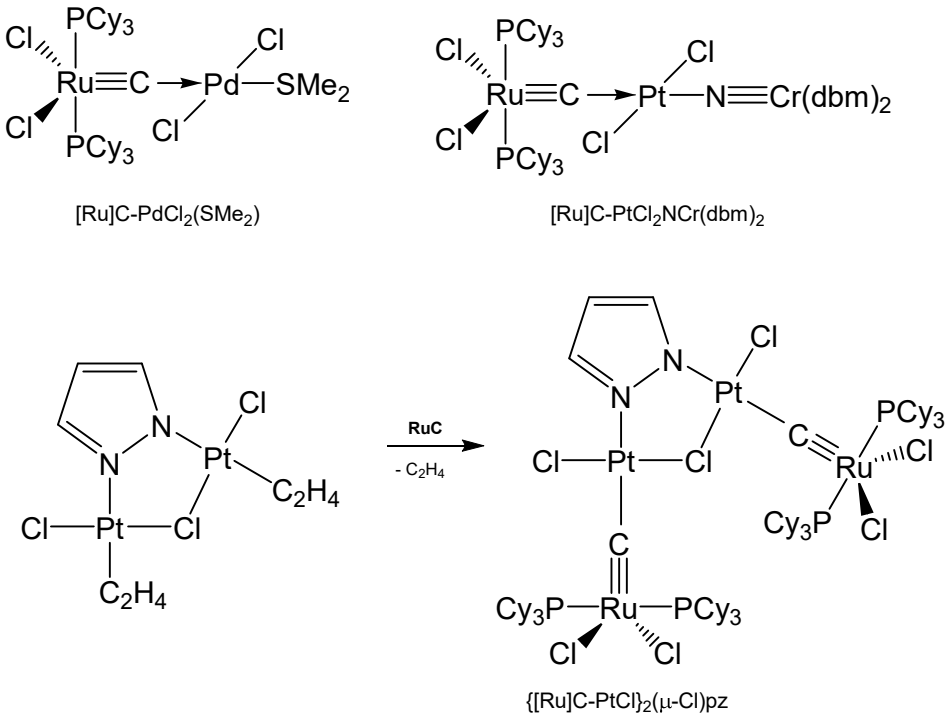

Scheme 26. Selected [Ru]C→M carbido complexes and synthesis of {[Ru]C→PtCl}$_2$(μ-Cl)pz

3.2. The system $RuCl_2(PCy_3)(NHC)C$ (^{NHC}[Ru]C)

The X-ray analysis of ^{NHC}[Ru]C exhibits a Ru-C distance of 1.605(2) Å. A signal at 471.5 ppm was attributed to the ligand carbon atom. No addition compounds were described so far [22].

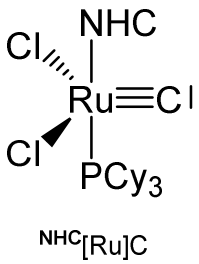

Figure 23. The ^{NHC}[Ru]C core

3.3. The system (NHC*)Cl_3RuC^- (NHC*[Ru]$^-$C)

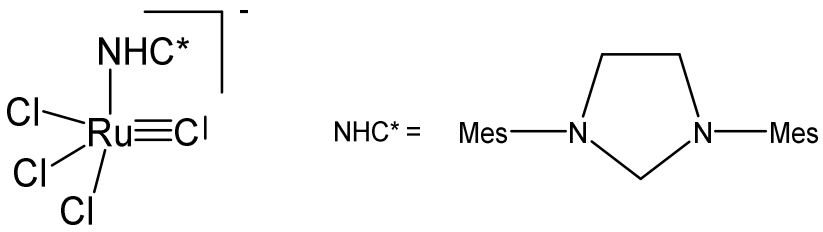

Figure 24. The $^{NHC*}[RuCl_3]^-$C core

Treating the carbene complex (NHC*)$Cl_2(PCy_3)Ru=CH_2$ at 55º in benzene generated the neutral complex depicted in Fig. 25. X-ray analysis revealed a Ru^1-C distance of 1.698(4) Å and the Ru^2-C distance of 1.875(4) Å with a Ru-C-Ru angle of 160.3(2)º. In the ^{13}C NMR the bridging C atom resonates at the typical value of 414.0 ppm.[123]

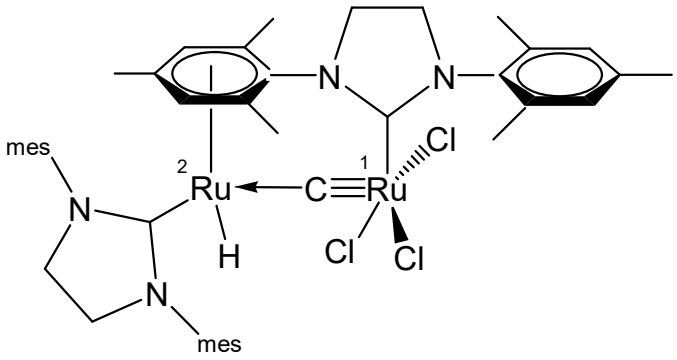

Figure 25. Structural representation of the Ru carbido complex $Ru_2(NHC*)_2Cl_3H$.

3.4. The system $RuClX(PCy_3)_2C$ ([Ru]XC)

Various carbido complexes were reported in which one or both chloride ions in [Ru]C are replaced by X (X = Br, I, CN, NCO, NCS). {[Ru](MeCN)C}OTf is the first cationic carbido complex which is also starting point for most of the substituted carbido complexes. X-ray data for {[Ru](MeCN)C}OTf, $[Ru](CN)_2C$, [Ru](Br)C, and [Ru](NCO)C are available [103].

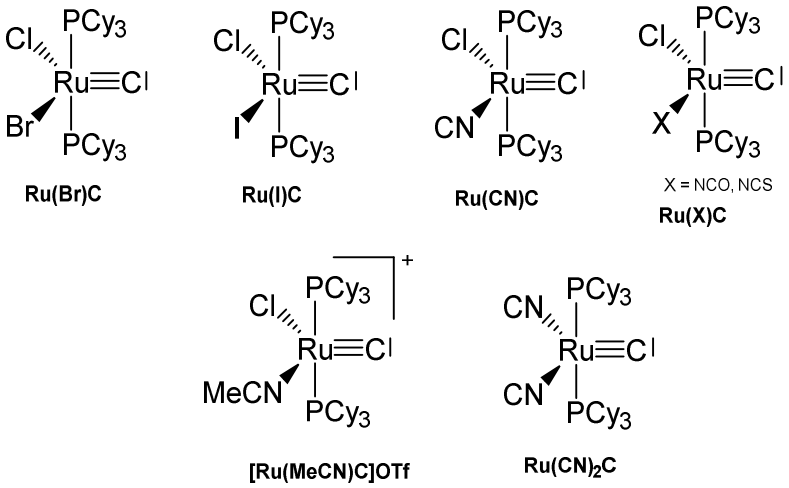

Figure 26. Carbido compounds of [Ru]XC with various X.

Table 16. Carbido complexes with the [Ru]XC core.

	^{13}C NMR	Ru-C	M-C	Ru-C-M	Ref
{[Ru](MeCN)C}OTf	464.75	nr	nr	nr	[103]
[Ru](CN)$_2$C	464.7	nr	nr	nr	[103]
[Ru](F)C	474.58	nr	nr	nr	[103]
[Ru](Br)C	471.38	nr	nr	nr	[103]
[Ru](I)C	469.74	nr	nr	nr	[103]
[Ru](CN)C	474.91	nr	nr	nr	[103]
[Ru](NCO)C	473.51	nr	nr	nr	[103]
[Ru](NCS)C	477.50	nr	nr	nr	[103]

3.5. The systems OsCl$_2$(PCy$_3$)$_2$C, OsI$_2$(PCy$_3$)$_2$C and OsCl$_2$(PCy$_3$)$_2$C ([OsX]C)

The carbido complexes [OsX]C were studied by X-ray analysis. The most important structural parameter is the Os-C separation, which for X = Cl amounts to 1.689(5) Å [104]. Single-crystal X-ray diffraction reveals that molecular [OsX]C adopts an approximately square-pyramidal core geometry, with the carbido ligand occupying the apical position and a short Os-C bond. In the ^{13}C NMR spectrum the signal at 471.8 ppm for X = Cl was attributed to the

ligand carbon atom. It was synthesized via S-atom abstraction from the thiocarbonyl complex $Os(CS)(PCy_3)_2Cl_2$ by $Ta(OSi\text{-}t\text{-}Bu_3)_3$. The diiodo derivative was synthesized from [OsCl]C upon reacting with 10 eq of Me_3SiI and exhibits a ^{13}C NMR signal at 446.14 ppm.

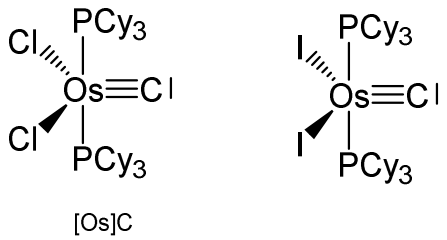

[Os]C

Figure 27. The [Os]C core

3.6. The system $[Tp^*Mo(CO)_3{\equiv}C]^+$ ($[Mo]^+C$)

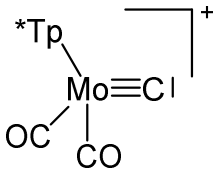

$[Mo]^+C$

*T = tris(3,5-dimethylpyrazolyl)borate

Figure 28. The $[Mo]^+C$ core.

The reaction between $Tp^*Mo(CO)_2CCl$ and $KFeCp(CO)_2$ generates the carbido complex $[Mo]C{\rightarrow}FeCp(CO)_2$ [105]. When $Tp^*Mo(CO)_2CSe$ was allowed to react with $[Ir(NCMe)(CO)(PPh_3)_2]BF_4$ the tetranuclear carbido complex $(\mu\text{-}Se_2)[Ir_2\text{-}\{[Mo]C\}_2(CO)_2(PPh_3)_2]$ was obtained, see Fig. 29 [106]. A solution of $Tp^*Mo(CO)_2CBr$ in THF was treated with BuLi followed by addition of $HgCl_2$ resulted in the formation of the carbido complex $[Mo]C{\rightarrow}Hg{\leftarrow}C[Mo]$ [107].

Table 17. Compounds with $[Mo]^{+}C$ core.

	Mo-C	M-C	Mo-C-M	^{13}C NMR	Ref
[Mo]C→$FeCp(CO)_2$	1.819(6)	1.911(8)	172.2(5)	381	[105]
(μ-Se_2)[Ir_2-{[Mo]C}$_2$$(CO)_2(PPh_3)_2$]	1.843(5)	1.974(5)	171.3(3) 168.2(3)	286.1	[106]
[Mo]C→Hg←C[Mo]	nr	nr	nr	373	[107]
[Mo]C→$AuPPh_3$	nr	nr	nr	nr	[108]

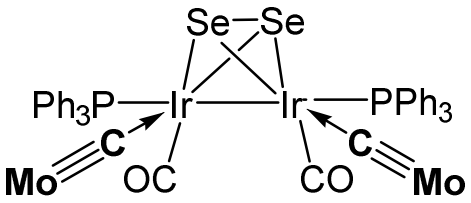

Figure 29. Selected structures of compounds with the $[Mo]^{+}C$ moiety.

3.7. Unique Mo carbido complex

A further unique carbido complex was described recently as shown in Fig. 28. A signal at 360.8 ppm in the ^{13}C NMR spectrum was assigned to the ligand carbon atom [109].

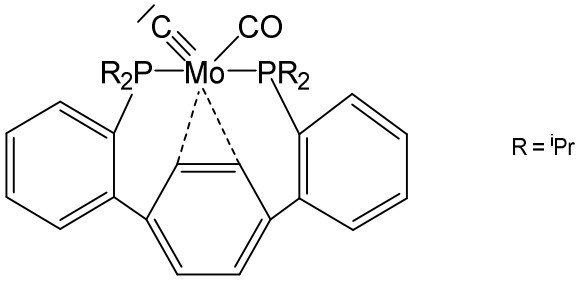

Figure 30. The carbido complex with the $P_2(CO)Mo{\equiv}C$ core.

3.8. The system [Tp*W(CO)$_3$≡C]$^+$ ([W]$^+$C)

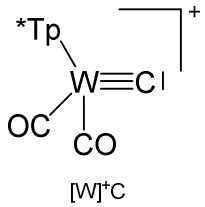

Figure 31. The [W]$^+$C core

Reaction of [W]C-Li(THF) with $NiCl_2(PEt_3)_2$ produced the complex [W]C→$NiCl(PEt_3)_2$ [110]. Similarly, with [W]C-Li(THF) and $FeCl(CO)_2Cp$ or $HgCl_2$ the compounds [W]C→$Fe(CO)_2Cp$ and [W]C→Hg←C[W], respectively, were obtained. [W]C→$AuPEt_3$ was prepared from reacting [W]C→$SnMe_3$ with $AuCl(SMe_2)$ followed by addition of PEt_3. A similar reaction with $AuCl(PPh_3)$ yielded [W]C→$AuPPh_3$. [W]C→$AuAsPh_3$ and [W]C→$AuPPh_3$ form a tetrameric assembly as depicted in Fig. 32. The X-ray analysis of the tetrameric unit revealed Au-C distances of 1.995 and 2.078 Å and a W-C distances of 1.877 Å [108].

Table 18. Compounds with [W]$^+$C core.

	W-C	M-C	W-C-M	^{13}C NMR	Ref
[W]C→$NiCl(PEt_3)_2$	nr	nr	nr	nr	[110]
[W]C→$Fe(CO)_2Cp$	nr	nr	nr	nr	[108]
[W]C→Hg←C[W]	nr	nr	nr	nr	[108]
[W]C→$AuAsPh_3$	nr	nr	nr	nr	[108]
[W]C→$AuPPh_3$	nr	nr	nr	nr	[108]
[W]C→$AuPEt_3$	nr	nr	nr	397.7	[108]

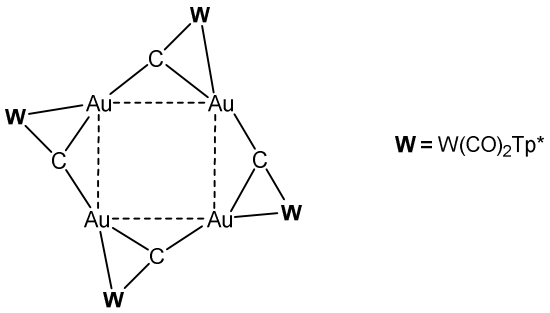

Figure 32. Tetrameric unit from [W]C→AuAsPh$_3$ and [W]C→AuPPh$_3$ [108].

3.9. The systems N$_3$MoC and O$_3$MoC

The potassium salt of ^{N}**MOC**$^{-}$ is dimeric with two K^+ ions bridging two anions and can be transformed with the crown ethers 2.0-benzo-15-crown-5 and 1.0 2,2,2-crypt into the related ion pairs. X-ray analysis of the crown ether salt revealed a Mo-C distance of 1.713(9) Å [21,111].

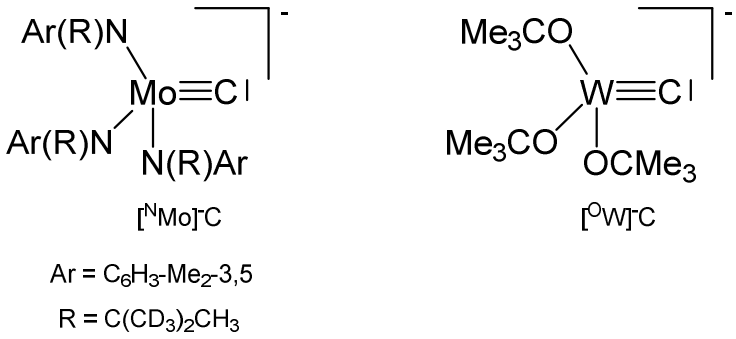

Figure 33. The [^{N}Mo]$^{-}$C and [^{O}W]$^{-}$C core.

The complex [^{O}W]C→Ru(CO)$_2$Cp was prepared from reacting [^{O}W]C-Et with Ru(C≡CMe)(CO)$_2$Cp under loss of MeCCEt. The ligand C atom resonates at 237.3 ppm ($^1J_{WC}$ = 290.1 Hz). Distances are W-C = 1.75(2) Å, Ru-C = 2.09(2) Å and the W-C-Ru angle amounts to 177(2) º [112].

3.10. Symmetrically bridged carbido complexes M=C=M

3.10.1. The Fe=C=Fe core

[Fe(TPP)]$_2$C was obtained from Fe^{III}(TPP)Cl in the presence of iron powder by reacting with CI_4 (TPP = 5, 10, 15, 20-tetraphenylporphyrin; according to Fe^{II} the complex is diamagnetic [113] X-ray analysis revealed an Fe-C bond length of 1.675 Å and a Fe-C-Fe angle of 180º [114].

[Fe(pc)(1-meim)}$_2$C was similarly obtained as the Tpp derivate; starting with pcFe and CI_4 followed by addition of sodium dithionite gave the μ-carbido bridged dimer; the Fe-C bond distance amounts to 1.70(1) Å and the Fe-C-Fe angle is 178(1) º (1-meim = 1-methylimidazole, pc = phthalocyanine) [115].

3. 10.2. The Rh=C=Rh core

[Rh(PEt$_3$)$_2$(SGePh$_3$)]$_2$C was obtained upon reacting Rh(PEt$_3$)$_2$(SGePh$_3$)CS with Rh(PEt$_3$)$_3$(Bpin) via the intermediate mixed carbido complex (SGePh$_3$)(PEt$_3$)$_2$Rh=C=Rh(PEt$_3$)$_2$(SBpin) which rearranges to this complex and [Rh(PEt$_3$)$_2$(SBpin)]$_2$. The X-ray analysis was performed (see Table 19) [116] [Rh(PEt$_3$)$_2$(SBpin)]$_2$C was prepared earlier by the same working group from Rh(PEt$_3$)$_3$(Bpin) and 0,5 eq of CS_2 (X-ray data see Table 19). Addition of MeOH generated the carbido complex [Rh(PEt$_3$)$_2$(SH)]$_2$C [117]. [Rh(Cl)(PPh$_3$)$_2$]$_2$C resulted from reacting the thiocarbonyl complex Rh(Cl)(PPh$_3$)$_2$CS with HBCat. The central C atom resonates at 424 ppm (t, $^1J_{RhC}$ = 47 Hz). In the chloro complex the chloride ion can be replaced with K[(H$_2$B(pz)$_2$], K[(H$_2$B(pzMe$_2$)$_2$], or K[(HB(pz)$_3$] to produce the carbido complexes [Rh(H$_2$B(pz)$_2$)(PPh$_3$)]$_2$C, [Rh(H$_2$B(pzMe$_2$)$_2$)(PPh$_3$)]$_2$C, and [Rh(HB(pz)$_3$)(PPh$_3$)]$_2$C, respectively. The unusual asymmetric carbido complex [Rh$_2$H(μ-C)(μ-C$_6$H$_4$PPh$_2$-2){HB(pzMe$_2$)$_3$}$_2$] contains a Rh^I atom with a shorter Rh-C distance, while the Rh^{III} –C distance is longer [118].

Table 19. Rh-C distances (in Å) and Rh-C-Rh angles (in deg). ^{13}C NMR of the bridging carbon atom in ppm.

	^{13}C NMR	Rh-C	Rh-C	Rh-C-Rh	Ref
$[Rh(PEt_3)_2(SGePh_3)]_2C$	425.8 $^1J_{RhC} = 47$	1.788(4)	1.798(4)	175.6(2)	[116]
$[Rh(PEt_3)_2(SBpin)]_2C$	nr	1.790(7)	1.766(7)	176.1(4)	[116,117]
$[Rh(PEt_3)_2(SH)]_2C$	nr	nr	nr	nr	[117]
$[Rh(Cl)(PPh_3)_2]_2C$	424 t, $^1J_{RhC} = 47$	1.7828(19)	1.7828(19)		[118]
$[Rh(H_2B(pz)_2)(PPh_3)]_2C$	nr	1.7644(11)	1.7644(11)	169.1(7)	[118]
$[Rh(H_2B(pzMe_2)_2)(PPh_3)]_2C$	nr	1.7794(9)	1.7794(9)	168.8(6)	[118]
$[Rh(HB(pz)_3)(PPh_3)]_2C$	nr	1.7761(7)	1.7761(7)	163.7(4)	[118]
$[Rh_2H(\mu\text{-}C)(\mu\text{-}C_6H_4PPh_2\text{-}2)\{HB(pzMe_2)_3\}_2]$	447.2 $^1J_{RhC} = 40$, 50	1.740(6) Rh^I	1.818(6) Rh^{III}	165.9(3)	[118]

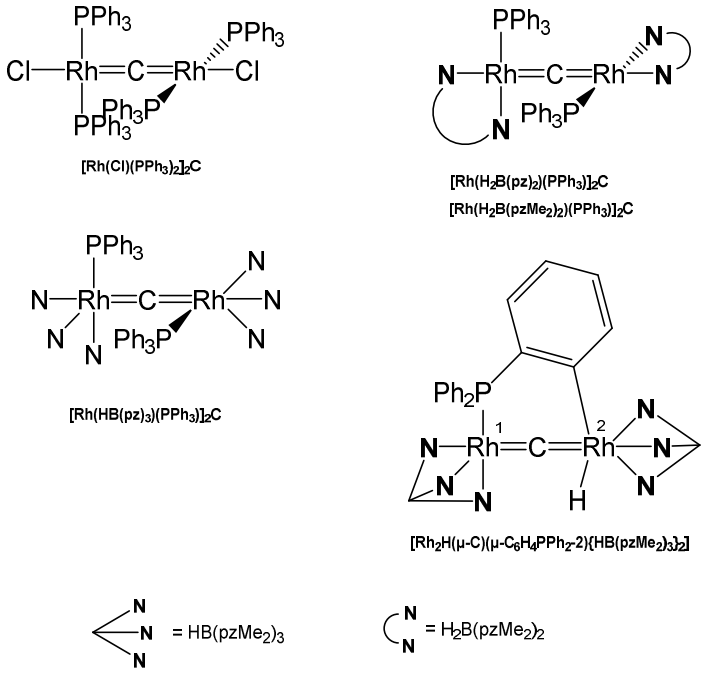

Figure 34. Selected structures of Rh=C=Rh complexes.

3.10.3. The Ru=C=Ru core

The tetranuclear carbido complex $[Ru(PEt_3)Cl(\mu\text{-}Cl_3)RuAr]_2C$ was prepared from the reaction of $[(p\text{-cymene})Ru(\mu\text{-}Cl)_3RuCl(C_2H_4)\text{-}(PCy_3)]$ with HCCH in THF. X-ray analysis adopts Ru-C distances of 1.877(9) Å and a Ru-C-Ru angle of 178.8(9)º [119].

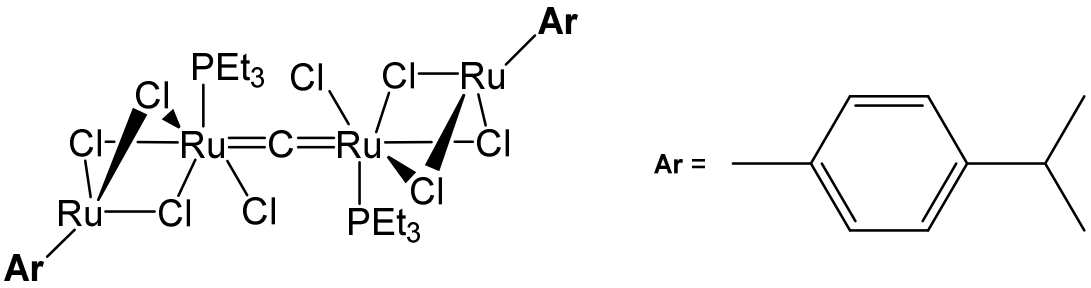

$[Ru(PEt_3)Cl(\mu\text{-}Cl_3)RuAr]_2C$

Figure 35. Structural representation of the Ru carbido complex $[Ru(PEt_3)Cl(\mu\text{-}Cl_3)RuAr]_2C$.

3.10.4. The Re=C=Re core

The unique carbido complex **$[Re(CO)_2Cp]_2C$** results from reaction of $[Re(thf)(CO)_2(\eta\text{-}C_5H_5)]$, CS_2, and PPh_3 (with the aim of the thiocarbonyl complex $[Re(CS)(CO)(\eta\text{-}C_5H_5)]$) as by-product in small amounts. X-ray analysis revealed Re-C distances of 1.882(14) and 1.881(14) Å and a Re-C-Re angle of 173.3(7)º. A ^{13}C NMR shift for the ligand carbon atom at δ_C = 436.4 ppm was measured [120].

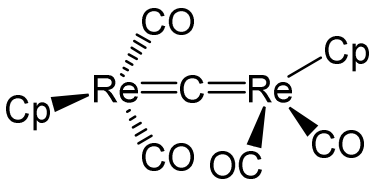

$[Re(CO)_2Cp]_2C$

Figure 36. Structural representation of the Re carbido complex $[Re(CO)_2Cp]_2C$.

3.11. Asymmetrically bridged carbido complex M'=C=M

3.11.1. The Fe=C=Re core

The asymmetrical carbido complex (TPP)Fe=C=Re(CO)$_4$Re(CO)$_5$ was prepared upon reacting the dichlorocarbene complex (TPP)Fe=CCl$_2$ with 2 eq of pentacarbonylrhenate, [Re(CO)$_5$]$^-$, under release of CO and 2 Cl$^-$; TPP is tetraphenylporphyrin. Crystals were analyzed by X-ray diffraction and revealed a Fe=C distance of 1.605(13) Å and a C=Re distance of 1.957(12) Å. The Fe-C-Re angle amounts to 173.3(9) º; the Fe-C distance is somewhat smaller than in [(TPP)Fe]$_2$C and the Re-C distance is appreciable longer than in [Re(CO)$_2$Cp]$_2$C. In the ^{13}C NMR spectrum the central carbido C atom resonates at 211.7 ppm [122]

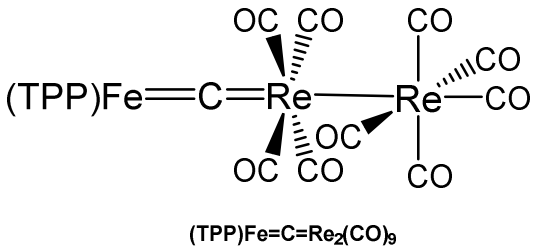

(TPP)Fe=C=Re$_2$(CO)$_9$

Figure 37. Structural representation of the Fe=C=Re carbido complex (TPP)Fe=C=Re$_2$(CO)$_9$.

4. Conclusion

The experimental and theoretical research about transition metal complexes with carbone ligands [M]-CL$_2$ and carbido complexes [M]-C has blossomed in the recent past and it can be foreseen that it will remain a very active area of organometallic chemistry in the future. The well-known family of transition metal complexes with C1-bonded carbon ligands that comprise alkyl (CR$_3$), carbene (CR$_2$) and carbyne (CR) groups has been extended by carbones (CL$_2$) and carbido (C) ligands. The summary of recent work, which is described in this review, indicates that carbone and carbido complexes are still largely terra incognita and that many new discoveries can be expected.

Author contributions: Conceptualization and writing of the first draft, W.P. and G.F. Checking and partial visualization L.Z. and C.C. All authors have read and agreed to the published version of the manuscript.

Funding: The work at Marburg was financially supported by the Deutsche Forschungsgemeinschaft. L.Z. and G.F acknowledge the financial support from Nanjing Tech University (grant number 39837132 and 39837123), National Natural Science Foundation of China (Grant No. 21703099 and 21993044), Natural Science Foundation of Jiangsu Province for Youth (Grant No: BK20170964), and SICAM Fellowship from Jiangsu National Synergetic Innovation Center for Advanced Materials.

Conflicts of Interest: The authors declare no conflict of interest.

References

1. Frankland, E. Über die Isolierung der organischen Radicale. *Justus Liebigs Ann. Chem.* **1849**, *71*, 171-213.
2. Seyferth, D. Zinc Alkyls, Edward Frankland, and the Beginnings of Main-Group Organometallic Chemistry. *Organometallics*. **2001**, *20*, 2940-2955.
3. Fischer, E. O. M., A Zur Frage eines Wolfram-Carbonyl-CarbenKomplexes. *Angew. Chem*. **1964**, *76*, 645.
4. Fischer, E. O.; Kreis, G.; Kreiter, C. G.; Müller, J.; Huttner, G.; Lorenz, H. trans-Halogeno[alkyl(aryl)carbyne]tetracarbonyl Complexes of Chromium, Molybdenum, and Tungsten —A New Class of Compounds Having a Transition Metal-Carbon Triple Bond. *Angew. Chem. Int. Ed.* **1973**, *12*, 564-565.
5. Schrock, R. R. Alkylcarbene complex of tantalum by intramolecular .alpha.-hydrogen abstraction. *J. Am. Chem. Soc.* **1974**, *96*, 6796-6797.
6. McLain, S. J.; Wood, C. D.; Messerle, L. W.; Schrock, R. R.; Hollander, F. J.; Youngs, W. J.; Churchill, M. R. Multiple metal-carbon bonds. 10. Thermally stable tantalum alkylidyne complexes and the crystal structure of Ta(.eta.5-C5Me5)(CPh)(PMe3)2Cl. *J. Am. Chem. Soc.* **1978**, *100*, 5962-5964.
7. Dewar, M. J. S. A review of Π Complex Theory. *Bull. Soc. Chim. Fr.* **1951**, *18*, C79.
8. Chatt, J.; Duncanson, L. A. 586. Olefin co-ordination compounds. Part III. Infra-red spectra and structure: attempted preparation of acetylene complexes. *J. Chem. Soc.* **1953**, 2939-2947.
9. Vyboishchikov, S. F.; Frenking, G. Theoretical studies of organometallic compounds, part 29 - Structure and bonding of low-valent (Fischer-type) and high-valent (Schrock-type) transition metal carbene complexes. *Chem. Eur. J.* **1998**, *4*, 1428-1438.
10. Vyboishchikov, S. F.; Frenking, G. Structure and Bonding of Low-Valent (Fischer-Type) and High-Valent (Schrock-Type) Transition Metal Carbyne Complexes. *Chem. Eur. J.* **1998**, *4*, 1439-1448.
11. Jerabek, P.; Schwerdtfeger, P.; Frenking, G. Dative and electron-sharing bonding in transition metal compounds. *J. Comput. Chem.* **2019**, *40*, 247-264.
12. Frenking, G.; Tonner, R. Divalent carbon(0) compounds. *Pure Appl. Chem.* **2009**, *81*, 597-614.
13. Frenking, G.; Tonner, R.; Klein, S.; Takagi, N.; Shimizu, T.; Krapp, A.; Pandey, K. K.; Parameswaran, P. New bonding modes of carbon and heavier group 14 atoms Si–Pb. *Chem. Soc. Rev.* **2014**, *43*, 5106-5139.
14. Frenking, G.; Hermann, M.; Andrada, D. M.; Holzmann, N. Donor–acceptor bonding in novel low-coordinated compounds of boron and group-14 atoms C–Sn. *Chem. Soc. Rev.* **2016**, *45*, 1129-1144.

15. Stable carbene complexes have a partially filled p(π) AO through π backdonation from the substituents R.
16. Tonner, R.; Heydenrych, G.; Frenking, G. First and Second Proton Affinities of Carbon Bases. *ChemPhysChem*. **2008**, *9*, 1474-1481.
17. Jensen, P.; Johns, J. W. C. The infrared spectrum of carbon suboxide in the ν6 fundamental region: Experimental observation and semirigid bender analysis. *J. Mol. Spectrosc.* **1986**, *118*, 248-266.
18. Koput, J. An ab initio study on the equilibrium structure and CCC bending energy levels of carbon suboxide. *Chem. Phys. Lett.* **2000**, *320*, 237-244.
19. Tonner, R.; Frenking, G. Divalent Carbon(0) Chemistry, Part 1: Parent Compounds. *Chem. Eur. J.* **2008**, *14*, 3260-3272.
20. Frenking, G. Dative Bonds in Main-Group Compounds: A Case for More Arrows! *Angew. Chem. Int. Ed.* **2014**, *53*, 6040-6046.
21. Peters, J. C.; Odom, A. L.; Cummins, C. C. A terminal molybdenum carbide prepared by methylidyne deprotonation. *Chem. Commun.* **1997**, 1995-1996.
22. Carlson, R. G.; Gile, M. A.; Heppert, J. A.; Mason, M. H.; Powell, D. R.; Velde, D. V.; Vilain, J. M. The Metathesis-Facilitated Synthesis of Terminal Ruthenium Carbide Complexes: A Unique Carbon Atom Transfer Reaction. *J. Am. Chem. Soc.* **2002**, *124*, 1580-1581.
23. Krapp, A.; Pandey, K. K.; Frenking, G. Transition Metal−Carbon Complexes. A Theoretical Study. *J. Am. Chem. Soc.* **2007**, *129*, 7596-7610.
24. Reinholdt, A.; Bendix, J. Platinum(ii) as an assembly point for carbide and nitride ligands. *Chem. Commun.* **2019**, *55*, 8270-8273.
25. Ramirez, F.; Desai, N. B.; Hansen, B.; McKelvie, N. HEXAPHENYLCARBODIPHOSPHORANE, (C6H5)3PCP(C6H5)3. *J. Am. Chem. Soc.* **1961**, *83*, 3539-3540.
26. Hussain, M. S.; Schmidbaur, H. Ein gemischt methyl/phenyl-substituiertes Carbodiphosphoran. Darstellung, Reaktionen und verwandte Verbindungen. *Z. Naturforsch*. **1976**, *31b*, 721-726.
27. Kroll, A.; Steinert, H.; Scharf, L. T.; Scherpf, T.; Mallick, B.; Gessner, V. H. A diamino-substituted carbodiphosphorane as strong C-donor and weak N-donor: isolation of monomeric trigonal-planar L·ZnCl2. *Chem. Commun.* **2020**, *56*, 8051-8054.
28. Quinlivan, P. J.; Parkin, G. Flexibility of the Carbodiphosphorane, (Ph3P)2C: Structural Characterization of a Linear Form. *Inorg. Chem.* **2017**, *56*, 5493-5497.
29. Vincent, A. T.; Wheatley, P. J. Crystal structure of bis(triphenylphosphoranylidene)methane [hexaphenylcarbodiphosphorane, Ph3P:C:PPh3]. *J. Chem. Soc., Dalton Trans.* **1972**, 617-622.

30. Schmidbaur, H.; Hasslberger, G.; Deschler, U.; Schubert, U.; Kappenstein, C.; Frank, A. PROBLEM OF THE STRUCTURE OF CARBODIPHOSPHORANES, R3PCPR3 - NEW ASPECTS. *Angew. Chem. Int. Ed.* **1979**, *18*, 408-409.
31. Schubert, U.; Kappenstein, C.; Milewskimahrla, B.; Schmidbaur, H. MOLECULAR AND CRYSTAL-STRUCTURES OF 2 CARBODIPHOSPHORANES WITH P-C-P BOND ANGLES NEAR 120-DEGREES. *Chem. Ber. Recl.* **1981**, *114*, 3070-3078.
32. Schmidbaur, H.; Costa, T.; Milewskimahrla, B.; Schubert, U. RING-STRAINED CARBODIPHOSPHORANES. *Angew. Chem. Int. Ed.* **1980**, *19*, 555-556.
33. Dorta, R.; Stevens, E. D.; Scott, N. M.; Costabile, C.; Cavallo, L.; Hoff, C. D.; Nolan, S. P. Steric and Electronic Properties of N-Heterocyclic Carbenes (NHC): A Detailed Study on Their Interaction with Ni(CO)4. *J. Am. Chem. Soc.* **2005**, *127*, 2485-2495.
34. Pugh, D.; Wright, J. A.; Freeman, S.; Danopoulos, A. A. 'Pincer' dicarbene complexes of some early transition metals and uranium. *Dalton Trans.* **2006**, 775-782.
35. Gardner, B. M.; McMaster, J.; Liddle, S. T. Synthesis and structure of a bis-N-heterocyclic carbene complex of uranium tetrachloride exhibiting short Cl···Ccarbene contacts. *Dalton Trans.* **2009**, 6924-6926.
36. Petz, W.; Weller, F.; Uddin, J.; Frenking, G. Reaction of carbodiphosphorane Ph3P=C=PPh3 with Ni(CO)(4). Experimental and theoretical study of the structures and properties of (CO)(3)NiC(PPh3)(2) and (CO)(2)NiC(PPh3)(2). *Organometallics*. **1999**, *18*, 619-626.
37. Petz, W.; Neumuller, B. Reaction of C(PPh3)(2) with MI2 Compounds (M = Zn, Cd) - Formation and Crystal Structures of I2Zn{C(PPh3)(2)} , (I2Cd{C(PPh3)(2)})(2) and the Salt-Like Compounds (HC{PPh3}(2)) MI3(THF) and (HC{PPh3}(2))(2) ZnI4. *Eur. J. Inorg. Chem.* **2011**, 4889-4895.
38. Petz, W.; Neumüller, B.; Klein, S.; Frenking, G. Syntheses and Crystal Structures of [Hg{C(PPh3)2}2][Hg2I6] and [Cu{C(PPh3)2}2]I and Comparative Theoretical Study of Carbene Complexes [M(NHC)2] with Carbone Complexes [M{C(PH3)2}2] (M = Cu+, Ag+, Au+, Zn2+, Cd2+, Hg2+). *Organometallics*. **2011**, *30*, 3330-3339.
39. Petz, W.; Öxler, F.; Neumüller, B. Syntheses and crystal structures of linear coordinated complexes of Ag+ with the ligands C(PPh3)2 and (HC{PPh3}2)+. *J. Organomet. Chem.* **2009**, *694*, 4094-4099.
40. Sundermeyer, J.; Weber, K.; Peters, K.; von Schnering, H. G. Modeling Surface Reactivity of Metal Oxides: Synthesis and Structure of an Ionic Organorhenyl Perrhenate Formed by Ligand-Induced Dissociation of Covalent Re2O7. *Organometallics*. **1994**, *13*, 2560-2562.

41. Schmidbaur, H.; Zybill, C. E.; Müller, G.; Krüger, C. Coinage Metal Complexes of Hexaphenylcarbodiphosphorane–Organometallic Compounds with Coordination Number 2. *Angew. Chem. Int. Ed.* **1983**, *22*, 729-730.
42. Zybill, C.; Mueller, G. Mononuclear complexes of copper(I) and silver(I) featuring the metals exclusively bound to carbon. Synthesis and structure of (.eta.5-pentamethylcyclopentadienyl)[(triphenylphosphonio)(triphenylphosphoranylidene)methyl]copper(I). *Organometallics*. **1987**, *6*, 2489-2494.
43. Vicente, J.; Singhal, A. R.; Jones, P. G. New Ylide−, Alkynyl−, and Mixed Alkynyl/Ylide−Gold(I) Complexes. *Organometallics*. **2002**, *21*, 5887-5900.
44. Kaska, W. C.; Reichelderfer, R. F. The interaction of hexaphenylcarbodiphosphorane with iridium olefin cations. Metalation of coordinated ligands. *J. Organomet. Chem.* **1974**, *78*, C47-C50.
45. Munzer, J. E.; Ona-Burgos, P.; Arrabal-Campos, F. M.; Neumuller, B.; Tonner, R.; Fernandez, I.; Kuzu, I. Difluoroborenium Cation Stabilized by Hexaphenyl-Carbodiphosphorane: A Concise Study on the Molecular and Electronic Structure of (Ph3P)(2)C(sic)BF2 BF4. *Eur. J. Inorg. Chem.* **2016**, 3852-3858.
46. Pranckevicius, C.; Iovan, D. A.; Stephan, D. W. Three and four coordinate Fe carbodiphosphorane complexes. *Dalton Trans.* **2016**, *45*, 16820-16825.
47. Kneusels, N. J. H.; Münzer, J. E.; Flosdorf, K.; Jiang, D.; Neumüller, B.; Zhao, L.; Eichhöfer, A.; Frenking, G.; Kuzu, I. Double donation in trigonal planar iron–carbodiphosphorane complexes – a concise study on their spectroscopic and electronic properties. *Dalton Trans.* **2020**, *49*, 2537-2546.
48. Su, W.; Pan, S.; Sun, X.; Wang, S.; Zhao, L.; Frenking, G.; Zhu, C. Double dative bond between divalent carbon(0) and uranium. *Nat. Commun.* **2018**, *9*, 4997.
49. Tonner, R.; Oexler, F.; Neumuller, B.; Petz, W.; Frenking, G. Carbodiphosphoranes: The chemistry of divalent Carbon(0). *Angew. Chem. Int. Ed.* **2006**, *45*, 8038-8042.
50. Flosdorf, K.; Jiang, D. D.; Zhao, L. L.; Neumuller, B.; Frenking, G.; Kuzu, I. An Experimental and Theoretical Study of the Structures and Properties of CDPMe-Ni(CO)(3) and Ni-2(CO)(4)(mu(2)-CO)(mu(2)-CDPMe). *Eur. J. Inorg. Chem.* **2019**, *2019*, 4546-4554.
51. Romeo, I.; Bardají, M.; Concepción Gimeno, M.; Laguna, M. Gold(I) complexes containing the cationic ylide ligand bis(methyldiphenylphosphonio)methylide. *Polyhedron*. **2000**, *19*, 1837-1841.
52. Bruce, A. E.; Gamble, A. S.; Tonker, T. L.; Templeton, J. L. Cationic phosphonium carbyne and bis(phosphonium) carbene tungsten complexes: [Tp'(OC)2WC(PMe_3)n][PF_6] (n = 1, 2). *Organometallics*. **1987**, *6*, 1350-1352.
53. Doddi, A.; Gemel, C.; Seidel, R. W.; Winter, M.; Fischer, R. A. Coordination complexes of TiX4 (X=F, Cl) with a bulky N-heterocyclic carbene: Syntheses, characterization and molecular structures. *Polyhedron*. **2013**, *52*, 1103-1108.

54. Datt, M. S.; Nair, J. J.; Otto, S. Synthesis and characterisation of two novel Rh(I) carbene complexes: Crystal structure of [Rh(acac)(CO)(L1)]. *J. Organomet. Chem.* **2005**, *690*, 3422-3426.
55. Stallinger, S.; Reitsamer, C.; Schuh, W.; Kopacka, H.; Wurst, K.; Peringer, P. Novel route to carbodiphosphoranes producing a new P,C,P pincer carbene ligand. *Chem. Commun.* **2007**, 510-512.
56. Klein, M.; Xie, X.; Burghaus, O.; Sundermeyer, J. Synthesis and Characterization of a N,C,N-Carbodiphosphorane Pincer Ligand and Its Complexes. *Organometallics*. **2019**, *38*, 3768-3777.
57. Reitsamer, C.; Stallinger, S.; Schuh, W.; Kopacka, H.; Wurst, K.; Obendorf, D.; Peringer, P. Novel access to carbodiphosphoranes in the coordination sphere of group 10 metals: template synthesis and protonation of PCP pincer carbodiphosphorane complexes of C(dppm)2. *Dalton Trans.* **2012**, *41*, 3503-3514.
58. Maser, L.; Herritsch, J.; Langer, R. Carbodiphosphorane-based nickel pincer complexes and their (de)protonated analogues: dimerisation, ligand tautomers and proton affinities. *Dalton Trans.* **2018**, *47*, 10544-10552.
59. Reitsamer, C.; Hackl, I.; Schuh, W.; Kopacka, H.; Wurst, K.; Peringer, P. Gold(I) and Gold(III) complexes of the [CH(dppm)2]+ and C(dppm)2 PCP pincer ligand systems. *J. Organomet. Chem.* **2017**, *830*, 150-154.
60. Su, W.; Pan, S.; Sun, X.; Zhao, L.; Frenking, G.; Zhu, C. Cerium–carbon dative interactions supported by carbodiphosphorane. *Dalton Trans.* **2019**, *48*, 16108-16114.
61. Kubo, K.; Jones, N. D.; Ferguson, M. J.; McDonald, R.; Cavell, R. G. Chelate and Pincer Carbene Complexes of Rhodium and Platinum Derived from Hexaphenylcarbodiphosphorane, Ph3PCPPh3. *J. Am. Chem. Soc.* **2005**, *127*, 5314-5315.
62. Petz, W.; Neumüller, B. New platinum complexes with carbodiphosphorane as pincer ligand via ortho phenyl metallation. *Polyhedron*. **2011**, *30*, 1779-1784.
63. Kubo, K.; Okitsu, H.; Miwa, H.; Kume, S.; Cavell, R. G.; Mizuta, T. Carbon(0)-Bridged Pt/Ag Dinuclear and Tetranuclear Complexes Based on a Cyclometalated Pincer Carbodiphosphorane Platform. *Organometallics*. **2017**, *36*, 266-274.
64. Lin, G.; Jones, N. D.; Gossage, R. A.; McDonald, R.; Cavell, R. G. A Tris(carbene) Pincer Complex: Monomeric Platinum Carbonyl with Three Bound Carbene Centers. *Angew. Chem. Int. Ed.* **2003**, *42*, 4054-4057.
65. Marrot, S.; Kato, T.; Gornitzka, H.; Baceiredo, A. Cyclic Carbodiphosphoranes: Strongly Nucleophilic σ-Donor Ligands. *Angew. Chem. Int. Ed.* **2006**, *45*, 2598-2601.
66. Corberán, R.; Marrot, S.; Dellus, N.; Merceron-Saffon, N.; Kato, T.; Peris, E.; Baceiredo, A. First Cyclic Carbodiphosphoranes of Copper(I) and Gold(I) and Their Application in the Catalytic Cleavage of X−H Bonds (X = N and O). *Organometallics*. **2009**, *28*, 326-330.

67. Yogendra, S.; Schulz, S.; Hennersdorf, F.; Kumar, S.; Fischer, R.; Weigand, J. J. Reductive Ring Opening of a Cyclo-Tri(phosphonio)methanide Dication to a Phosphanylcarbodiphosphorane: In Situ UV-Vis Spectroelectrochemistry and Gold Coordination. *Organometallics*. **2018**, *37*, 748-754.
68. Alcarazo, M.; Radkowski, K.; Mehler, G.; Goddard, R.; Fürstner, A. Chiral heterobimetallic complexes of carbodiphosphoranes and phosphinidene–carbene adducts. *Chem. Commun.* **2013**, *49*, 3140-3142.
69. Petz, W.; Kutschera, C.; Neumüller, B. Reaction of the Carbodiphosphorane Ph3PCPPh3 with Platinum(II) and -(0) Compounds: Platinum Induced Activation of C−H Bonds. *Organometallics*. **2005**, *24*, 5038-5043.
70. Baldwin, J. C.; Kaska, W. C. The interaction of hexaphenylcarbodiphosphorane with the trimethylplatinum(IV) cation. *Inorg. Chem.* **1979**, *18*, 686-691.
71. Melaimi, M.; Parameswaran, P.; Donnadieu, B.; Frenking, G.; Bertrand, G. Synthesis and Ligand Properties of a Persistent, All-Carbon Four-Membered-Ring Allene. *Angew. Chem. Int. Ed.* **2009**, *48*, 4792-4795.
72. Hackl, L.; Petrov, A. R.; Bannenberg, T.; Freytag, M.; Jones, P. G.; Tamm, M. Dimerisation of Dipiperidinoacetylene: Convenient Access to Tetraamino-1,3-Cyclobutadiene and Tetraamino-1,2-Cyclobutadiene Metal Complexes. *Chem. Eur. J.* **2019**, *25*, 16148-16155.
73. Pranckevicius, C.; Liu, L.; Bertrand, G.; Stephan, D. W. Synthesis of a Carbodicyclopropenylidene: A Carbodicarbene based Solely on Carbon. *Angew. Chem. Int. Ed.* **2016**, *55*, 5536-5540.
74. Tonner, R.; Frenking, G. C(NHC)2: Divalent Carbon(0) Compounds with N-Heterocyclic Carbene Ligands—Theoretical Evidence for a Class of Molecules with Promising Chemical Properties. *Angew. Chem. Int. Ed.* **2007**, *46*, 8695-8698.
75. Dyker, C. A.; Lavallo, V.; Donnadieu, B.; Bertrand, G. Synthesis of an Extremely Bent Acyclic Allene (A "Carbodicarbene"): A Strong Donor Ligand. *Angew. Chem. Int. Ed.* **2008**, *47*, 3206-3209.
76. Hsu, Y. C.; Shen, J. S.; Lin, B. C.; Chen, W. C.; Chan, Y. T.; Ching, W. M.; Yap, G. P. A.; Hsu, C. P.; Ong, T. G. Synthesis and Isolation of an Acyclic Tridentate Bis(pyridine)carbodicarbene and Studies on Its Structural Implications and Reactivities. *Angew. Chem. Int. Ed.* **2015**, *54*, 2420-2424.
77. Chen, W. C.; Hsu, Y. C.; Lee, C. Y.; Yap, G. P. A.; Ong, T. G. Synthetic Modification of Acyclic Bent Allenes (Carbodicarbenes) and Further Studies on Their Structural Implications and Reactivities. *Organometallics*. **2013**, *32*, 2435-2442.
78. Chen, W. C.; Shen, J. S.; Jurca, T.; Peng, C. J.; Lin, Y. H.; Wang, Y. P.; Shih, W. C.; Yap, G. P. A.; Ong, T. G. Expanding the Ligand Framework Diversity of Carbodicarbenes and Direct Detection of Boron Activation in the Methylation of Amines with CO2. *Angew. Chem. Int. Ed.* **2015**, *54*, 15207-15212.

79. Ruiz, D. A.; Melaimi, M.; Bertrand, G. Carbodicarbenes, Carbon(0) Derivatives, Can Dimerize. *Chem. Asian J.* **2013**, *8*, 2940-2942.
80. Liberman-Martin, A. L.; Grubbs, R. H. Ruthenium Olefin Metathesis Catalysts Featuring a Labile Carbodicarbene Ligand. *Organometallics*. **2017**, *36*, 4091-4094.
81. Chan, S. C.; Gupta, P.; Engelmann, X.; Ang, Z. Z.; Ganguly, R.; Bill, E.; Ray, K.; Ye, S. F.; England, J. Observation of Carbodicarbene Ligand Redox Noninnocence in Highly Oxidized Iron Complexes. *Angew. Chem. Int. Ed.* **2018**, *57*, 15717-15722.
82. Chen, W. C.; Shih, W. C.; Jurca, T.; Zhao, L. L.; Andrada, D. M.; Peng, C. J.; Chang, C. C.; Liu, S. K.; Wang, Y. P.; Wen, Y. S.; Yap, G. P. A.; Hsu, C. P.; Frenking, G.; Ong, T. G. Carbodicarbenes: Unexpected pi-Accepting Ability during Reactivity with Small Molecules. *J. Am. Chem. Soc.* **2017**, *139*, 12830-12836.
83. Shih, W. C.; Chiang, Y. T.; Wang, Q.; Wu, M. C.; Yap, G. P. A.; Zhao, L.; Ong, T. G. Invisible Chelating Effect Exhibited between Carbodicarbene and Phosphine through π–π Interaction and Implication in the Cross-Coupling Reaction. *Organometallics*. **2017**, *36*, 4287-4297.
84. Goldfogel, M. J.; Roberts, C. C.; Meek, S. J. Intermolecular Hydroamination of 1,3-Dienes Catalyzed by Bis(phosphine)carbodicarbene–Rhodium Complexes. *J. Am. Chem. Soc.* **2014**, *136*, 6227-6230.
85. Roberts, C. C.; Matías, D. M.; Goldfogel, M. J.; Meek, S. J. Lewis Acid Activation of Carbodicarbene Catalysts for Rh-Catalyzed Hydroarylation of Dienes. *J. Am. Chem. Soc.* **2015**, *137*, 6488-6491.
86. Fürstner, A.; Alcarazo, M.; Goddard, R.; Lehmann, C. W. Coordination Chemistry of Ene-1,1-diamines and a Prototype "Carbodicarbene". *Angew. Chem. Int. Ed.* **2008**, *47*, 3210-3214.
87. Burzlaff, H.; Voll, U.; Bestmann, H. J. Die Kristall- und Molekülstruktur des (2,2-Diäthoxyvinyliden)-triphenylphosphorans. *Chem. Ber.* **1974**, *107*, 1949-1956.
88. Alcarazo, M.; Lehmann, C. W.; Anoop, A.; Thiel, W.; Furstner, A. Coordination chemistry at carbon. *Nature. Chem.* **2009**, *1*, 295-301.
89. Troadec, T.; Wasano, T.; Lenk, R.; Baceiredo, A.; Saffon-Merceron, N.; Hashizume, D.; Saito, Y.; Nakata, N.; Branchadell, V.; Kato, T. Donor-Stabilized Silylene/Phosphine-Supported Carbon(0) Center with High Electron Density. *Angew. Chem. Int. Ed.* **2017**, *56*, 6891-6895.
90. Morosaki, T.; Wang, W. W.; Nagase, S.; Fujii, T. Synthesis, Structure, and Reactivities of Iminosulfane- and Phosphane-Stabilized Carbones Exhibiting Four-Electron Donor Ability. *Chem. Eur. J.* **2015**, *21*, 15405-15411.
91. Pascual, S.; Asay, M.; Illa, O.; Kato, T.; Bertrand, G.; Saffon-Merceron, N.; Branchadell, V.; Baceiredo, A. Synthesis of a mixed phosphonium-sulfonium bisylide R3P=C=SR2. *Angew. Chem. Int. Ed.* **2007**, *46*, 9078-9080.

92. Morosaki, T.; Iijima, R.; Suzuki, T.; Wang, W. W.; Nagase, S.; Fujii, T. Synthesis, Electronic Structure, and Reactivities of Two-Sulfur-Stabilized Carbones Exhibiting Four-Electron Donor Ability. *Chem. Eur. J.* **2017**, *23*, 8694-8702.
93. Morosaki, T.; Suzuki, T.; Wang, W. W.; Nagase, S.; Fujii, T. Syntheses, Structures, and Reactivities of Two Chalcogen-Stabilized Carbones. *Angew. Chem. Int. Ed.* **2014**, *53*, 9569-9571.
94. Fujii, T.; Ikeda, T.; Mikami, T.; Suzuki, T.; Yoshimura, T. Synthesis and structure of (MeN)Ph_2S = C = SPh_2(NMe). *Angew. Chem. Int. Ed.* **2002**, *41*, 2576-2578.
95. Morosaki, T.; Suzuki, T.; Fujii, T. Syntheses and Structural Characterization of Mono-, Di-, and Tetranuclear Silver Carbone Complexes. *Organometallics*. **2016**, *35*, 2715-2721.
96. Chen, Y.; Petz, W.; Frenking, G. Is It Possible to Synthesize a Low-Valent Transition Metal Complex with a Neutral Carbon Atom as Terminal Ligand? A Theoretical Study of (CO)4FeC. *Organometallics*. **2000**, *19*, 2698-2706.
97. Zhao, L.; von Hopffgarten, M.; Andrada, D. M.; Frenking, G. Energy decomposition analysis. *WIREs Comput. Mol. Sci.* **2018**, *8*, e1345.
98. Hejl, A.; Trnka, T. M.; Day, M. W.; Grubbs, R. H. Terminal ruthenium carbido complexes as σ-donor ligands. *Chem. Commun.* **2002**, 2524-2525.
99. Caskey, S. R.; Stewart, M. H.; Kivela, J. E.; Sootsman, J. R.; Johnson, M. J. A.; Kampf, J. W. Two Generalizable Routes to Terminal Carbido Complexes. *J. Am. Chem. Soc.* **2005**, *127*, 16750-16751.
100. Reinholdt, A.; Bendix, J. Weakening of Carbide–Platinum Bonds as a Probe for Ligand Donor Strengths. *Inorg. Chem.* **2017**, *56*, 12492-12497.
101. Reinholdt, A.; Vibenholt, J. E.; Morsing, T. J.; Schau-Magnussen, M.; Reeler, N. E. A.; Bendix, J. Carbide complexes as π-acceptor ligands. *Chem. Sci.* **2015**, *6*, 5815-5823.
102. Reinholdt, A.; Herbst, K.; Bendix, J. Delivering carbide ligands to sulfide-rich clusters. *Chem. Commun.* **2016**, *52*, 2015-2018.
103. Morsing, T. J.; Reinholdt, A.; Sauer, S. P. A.; Bendix, J. Ligand Sphere Conversions in Terminal Carbide Complexes. *Organometallics*. **2016**, *35*, 100-105.
104. Stewart, M. H.; Johnson, M. J. A.; Kampf, J. W. Terminal Carbido Complexes of Osmium: Synthesis, Structure, and Reactivity Comparison to the Ruthenium Analogues. *Organometallics*. **2007**, *26*, 5102-5110.
105. Etienne, M.; White, P. S.; Templeton, J. L. An agostic .mu.-methyne molybdenum-iron complex from protonation of a .mu.-carbide precursor, Tp'(CO)2Mo.tplbond.CFe(CO)2Cp. *J. Am. Chem. Soc.* **1991**, *113*, 2324-2325.
106. Cade, I. A.; Hill, A. F.; McQueen, C. M. A. Iridium−Molybdenum Carbido Complex via C−Se Activation of a Selenocarbonyl Ligand: (μ-Se2)[Ir2{C≡Mo(CO)2(Tp*)}2(CO)2(PPh3)2] (Tp* = hydrotris(dimethylpyrazolyl)borate). *Organometallics*. **2009**, *28*, 6639-6641.

107. Colebatch, A. L.; Cordiner, R. L.; Hill, A. F.; Nguyen, K. T. H. D.; Shang, R.; Willis, A. C. A Bis-Carbyne (Ethanediylidyne) Complex via the Catalytic Demercuration of a Mercury Bis(carbido) Complex. *Organometallics*. **2009**, *28*, 4394-4399.
108. Borren, E. S.; Hill, A. F.; Shang, R.; Sharma, M.; Willis, A. C. A Golden Ring: Molecular Gold Carbido Complexes. *J. Am. Chem. Soc.* **2013**, *135*, 4942-4945.
109. Buss, J. A.; Agapie, T. Mechanism of Molybdenum-Mediated Carbon Monoxide Deoxygenation and Coupling: Mono- and Dicarbyne Complexes Precede C–O Bond Cleavage and C–C Bond Formation. *J. Am. Chem. Soc.* **2016**, *138*, 16466-16477.
110. Hill, A. F.; Sharma, M.; Willis, A. C. Heterodinuclear Bridging Carbido and Phosphoniocarbyne Complexes. *Organometallics*. **2012**, *31*, 2538-2542.
111. Agapie, T.; Diaconescu, P. L.; Cummins, C. C. Methine (CH) Transfer via a Chlorine Atom Abstraction/Benzene-Elimination Strategy: Molybdenum Methylidyne Synthesis and Elaboration to a Phosphaisocyanide Complex. *J. Am. Chem. Soc.* **2002**, *124*, 2412-2413.
112. Latesky, S. L.; Selegue, J. P. Preparation and structure of [(Me$_3$CO)$_3$W.tplbond.C-Ru(CO)2(Cp)], a heteronuclear, .mu.2-carbide complex. *J. Am. Chem. Soc.* **1987**, *109*, 4731-4733.
113. Mansuy, D.; Lecomte, J. P.; Chottard, J. C.; Bartoli, J. F. Formation of a complex with a carbide bridge between two iron atoms from the reaction of (tetraphenylporphyrin)iron(II) with carbon tetraiodide. *Inorg. Chem.* **1981**, *20*, 3119-3121.
114. Goedken, V. L.; Deakin, M. R.; Bottomley, L. A. Molecular stereochemistry of a carbon-bridged metalloporphyrin: μ-carbido-bid(5,10,15,20-tetraphenylporphinatoiron). *J. Chem. Soc., Chem. Commun.* **1982**, 607-608.
115. Rossi, G.; Goedken, V. L.; Ercolani, C. μ-Carbido-bridged iron phthalocyanine dimers: synthesis and characterization. *J. Chem. Soc., Chem. Commun.* **1988**, 46-47.
116. Ahrens, T.; Schmiedecke, B.; Braun, T.; Herrmann, R.; Laubenstein, R. Activation of CS2 and COS at a Rhodium(I) Germyl Complex: Generation of CS and Carbido Complexes. *Eur. J. Inorg. Chem.* **2017**, 713-722.
117. Kalläne, S. I.; Braun, T.; Teltewskoi, M.; Braun, B.; Herrmann, R.; Laubenstein, R. Remarkable reactivity of a rhodium(i) boryl complex towards CO_2 and CS_2: isolation of a carbido complex. *Chem. Commun.* **2015**, *51*, 14613-14616.
118. Barnett, H. J.; Burt, L. K.; Hill, A. F. Simple generation of a dirhodium μ-carbido complex via thiocarbonyl reduction. *Dalton Trans.* **2018**, *47*, 9570-9574.
119. Solari, E.; Antonijevic, S.; Gauthier, S.; Scopelliti, R.; Severin, K. Formation of a ruthenium mu-carbide complex with acetylene as the carbon source. *Eur. J. Inorg. Chem.* **2007**, 367-371.
120. Young, R. D.; Hill, A. F.; Cavigliasso, G. E.; Stranger, R. [(μ-C){Re(CO)$_2$(η-C5H5)}$_2$]: A Surprisingly Simple Bimetallic Carbido Complex. *Angew. Chem. Int. Ed.* **2013**, *52*, 3699-3702.

121. Takemoto, S.; Matsuzaka, H. Recent advances in the chemistry of ruthenium carbido complexes. *Coord Chem. Rev*. **2012**, *256*, 574-588.

122. Beck, W.; Knauer, W,; Robl, C. Synthesis and structure of the novel μ-carbido complex [(TPP)Fe=C=Re(CO)$_4$Re(CO)$_5$]. *Angew. Chem. Int. Ed*. **1990,** *29*, 318-320.

123. Hong, S. H.; Day, M. W.; Grupps, R. H. Decomposition of a key intermediate in Ruthenium-Catalyzed olefin metatesis reactions. *J. Am. Chem. Soc.* **2004**, *126*, 7414-7415.

124. Schmidbaur, H.; Gasser, O.; The Ambident Ligand Properties of Bis(trimethylphosphoranylidene)methan. *Angew. Chem. Int. Ed*. **1976,** *15*, 502-503.